Green Chemistry

TUTORIAL REVIEW

View Article Online
View Journal | View Issue

Cite this: *Green Chem.*, 2025, **27**, 4898

Machine learning-driven design of single-atom catalysts for carbon dioxide valorization to high-value chemicals: a review of photocatalysis, electrocatalysis, and thermocatalysis

Xiangyu Wen, [a,b] Xiao Geng,[b] Guandong Su,[b,c] Yizheng Li, [d] Qidong Li,[e] Yuxuan Yi [f] and Lifen Liu *[b,c]

The pressing need for carbon-neutral technologies has driven extensive research into photocatalytic, electrocatalytic, and thermocatalytic CO_2 reduction, with highly efficient single-atom catalysts (SACs) due to their atomically dispersed active sites, tunable coordination environments, and well-defined electronic structures. Recent advances in SACs have demonstrated enhanced activity, selectivity and stability through rational design strategies incorporating transition-metal-based single-atom sites, nitrogen-coordinated frameworks, and perovskite-, graphene-, or MOF-supports. Mechanistically, SACs facilitate CO_2 activation *via* optimized CO_2 adsorption, electronic-state modulation and selective stabilization of key intermediates, thus promoting tailored product formation. Despite significant progress, challenges remain in understanding the precise electronic effects governing intermediate binding and selectivity and suppressing metal aggregation under operando conditions. This review systematically integrates experimental findings with machine learning (ML)-assisted first-principles calculations, deep learning (DL) frameworks, and density functional theory (DFT) modeling to refine the performances of SACs. ML-driven Bayesian optimization accelerates catalyst discovery by correlating the synthesis parameters with reaction kinetics and thermodynamics. High-throughput experimental validation combined with multi-technique characterization elucidates the structure–activity relationships, providing insights into the electron transfer dynamics, coordination tuning, and catalytic site evolution. The integration of active learning algorithms enables self-optimizing SACs, dynamically adjusting synthesis and reaction conditions for superior selectivity and faradaic efficiency. By bridging predictive modeling with experimental validation, this review presents a comprehensive framework for the rational design of next-generation SACs, paving the way for high-efficiency conversion of CO_2 into valuable chemicals. The synergy between AI-driven catalyst discovery and mechanistic elucidation represents a paradigm shift toward viable and selective CO_2 valorization strategies.

Received 11th February 2025,
Accepted 6th March 2025

DOI: 10.1039/d5gc00739a

rsc.li/greenchem

Green foundation

1. This review discusses advancements in green chemistry, particularly in the CO_2 reduction reaction (CO_2RR) using single-atom catalysts (SACs). Key developments include the use of SACs for photocatalysis, electrocatalysis, and thermocatalysis, with improved CO_2 activation, enhanced selectivity, and increased efficiency through atomic-level precision.
2. The integration of experimental techniques with machine learning (ML), deep learning models (DL), and DFT establishes a data-driven framework for optimizing the design of SACs. This approach facilitates the iterative refinement of the catalyst properties, prediction of reaction pathways, and enhancement of efficiency and selectivity, thereby generating wider interest.
3. The future of this field lies in achieving a comprehensive understanding of mechanisms and refining SAC design through ML/DL/DFT and experimental validation. These insights will guide the rational development of SACs with enhanced performance, aiding the scalability of CO_2 reduction technologies and contributing to sustainability.

[a]*State Key Laboratory of Chemical Engineering, Zhejiang University, 310027 Hangzhou, China*
[b]*Key Laboratory of Industrial Ecology and Environmental Engineering (MOE), Dalian University of Technology, 116024 Liaoning, China. E-mail: lifenliu@dlut.edu.cn*
[c]*Department of Environment and Food, School of Chemical Engineering, Ocean, and Life Sciences, Dalian University of Technology, Panjin, 124221, China*
[d]*Department of Building Environment and Energy Engineering, The Hong Kong Polytechnic University, 999077 Hong Kong, China*
[e]*School of Engineering, The University of British Columbia, BC V1 V 1 V7, 1137 Alumni Ave, Kelowna, Canada*
[f]*College of Design and Engineering, National University of Singapore, 117575, Singapore*

1 Introduction

Rapid industrialization has greatly increased CO_2 emissions, intensifying the greenhouse effect and creating various social, ecological and environmental challenges. China's rising share in global emissions has spurred efforts for "dual carbon" goals, emphasizing the need for effective solutions like catalytic CO_2 reduction technologies. These technologies enable CO_2 conversion into valuable small organic molecules *via* thermocatalysis, electrocatalysis,[1–4] and photocatalysis,[5] offering promising pathways for CO_2 capture, storage (CCS), and utilization (CCU).[6,7] Thermocatalysis at high temperatures can activate CO_2, breaking C–O bonds and thereby producing C_1 and C_2 products. Meanwhile, in electrocatalysis,[8,9] CO_2 gets electrochemically reduced to form intermediates like formate, CO and methane;[10] in photocatalysis,[11] which mimics photosynthesis, light energy is used to generate charge carriers to activate and reduce CO_2.[12] These last two methods offer efficient solutions under mild conditions to reduce CO_2 emissions.[13] Converting CO_2 into high-value chemicals, such as CO, CH_4, HCOOH and C_2 compounds, is both a carbon utilization strategy and a focus area of CO_2RR for academic and industrial researchers.[14] The related progress is shown in the pivotal role of catalytic science and technology in driving advances in energy, environmental and industrial sectors, enhancing reaction efficiency and selectivity and lowering activation energies.[15] In recent years, the rapid progress of nanotechnology has propelled "nanocatalysts" to the forefront of energy, chemical, and environmental engineering owing to their high surface areas and unique catalytic properties.[16,17] Catalysts are designed to reduce the size of active metal components and to unveil the distinct catalytic effects at the nano-, sub-nano- and SAC-scale.[18] The concept of SACs was introduced while creating a Pt_1/FeO_x catalyst, where a single platinum atom was anchored on a ferrite nanocrystal.

SACs offer distinct advantages over traditional nanocatalysts, including exceptionally high atomic efficiency, large surface areas and well-defined, uniform active sites. These properties make SACs highly effective in catalytic applications such as organocatalysis,[19,20] photocatalysis[21,22] and electrocatalysis.[23,24] In CO_2RR, SACs, especially those incorporating Co, N and C (*e.g.*, M–N–C), exhibit superior performance due to their tailored coordination environments, enhanced electronic properties and precise control over the active site geometry. The high reactivity of these materials stems from their ability to fine-tune the electronic structure and optimize the catalytic pathway, facilitating efficient CO_2 activation and reduction to small organic molecules such as CO, formate, and methane. The mechanism involving CO_2 adsorption, activation *via* metal sites, electron transfer and bond cleavage, and formation of specific products, is determined by the catalyst's electronic structure and the reaction conditions.[25] Despite significant progress in the design of high-density, high-stability SACs, the underlying mechanisms and their transformation during reactions remain poorly understood. While SACs theoretically maximize atomic efficiency, the increased surface energy of the isolated metal atoms, due to their higher surface area, can lead to aggregation under reaction conditions. As the metal loading increases, SACs tend to cluster, leading to a loss of catalytic performance. Therefore, achieving both high stability and large substrate loading in SACs remains a major challenge. This issue is particularly relevant in CO_2RR, where maintaining the integrity of the isolated metal sites is crucial for efficient CO_2 activation and selective reduction to organic molecules. Hence, solutions for optimizing support materials, such as nitrogen-doped carbon frameworks, to stabilize isolated metal sites and prevent aggregation while maintaining their high reactivity and selectivity for CO_2RR[26] are highly desirable.

Prediction and optimization of SACs using ML have become key research directions, with recent major advancements in ML offering powerful tools for accelerating catalyst discovery,[27]

Xiangyu Wen

Mr Xiangyu Wen is currently pursuing a Master's degree in Chemical Engineering (Hydrogen Energy Science and Engineering) at Zhejiang University. His undergraduate research at Dalian University of Technology in 2024 focused on photocatalysis, electrocatalysis, and photoelectrocatalytic CO_2 reduction. Presently, his research is centered on the use of machine learning for catalyst design and thermocatalytic CO_2 reduction to produce high-value chemicals, with a commitment to advancing CCUS (Carbon Capture, Utilization, and Storage) and clean energy technologies.

Guandong Su

Dr Guandong Su is an Assistant Professor in the Department of Environment and Food, School of Chemical Engineering, Ocean, and Life Sciences, Dalian University of Technology. He received his PhD in Environmental Engineering from the National University of Singapore and B.Eng. in Petroleum Engineering from China University of Petroleum-Beijing in 2024 and 2018, respectively. His research interests lie in the interdisciplinary interface of energy and environment to advance sustainable development goals, with an emphasis on providing affordable and clean energy for the future.

fine-tuning reaction parameters, and unveiling complex reaction pathways.[28,29] A key advancement in photocatalysis is the development of NiNi heterobimetallic SACs, which outperform traditional catalysts by utilizing a redox-active ligand for CO_2 activation, highlighting the importance of dual-metal cooperation in catalyst design.[30] In electrocatalysis, ML-guided DFT calculations have optimized SACs, achieving low overpotentials and high CH_4 selectivity. Cu–Al catalysts, optimized *via* ML and DFT, show improved faradaic efficiency and selectivity, with active learning refining the reaction conditions such as the temperature and pressure.[31] Thermocatalysis has benefited from AI platforms like Carbon Copilot (CARCO), which accelerated the discovery of SACs for CO_2 conversion, achieving high precision in catalyst design within weeks.[32] Mechanistic studies using ML and *ab initio* calculations, such as with CuPt/TiO_2 catalysts, reveal that interface design is crucial for stabilizing CO_2 intermediates, further guiding the rational design of SACs.[33]

While existing reviews[34–36] have extensively covered the preparation methods, characterization techniques, auxiliary agents, and catalyst supports for SACs, there is a notable paucity of discussions on the synergistic optimization of ML/DL/DFT approaches alongside experimental strategies in the design of SACs, the identification of optimal reaction conditions, and the fine-tuning of SACs preparation parameters. In this context, our review offers a comprehensive analysis of the preparation methods, characterization techniques, mechanistic insights, reaction kinetics, and the integration of ML predictions for SACs in CO_2RR. We emphasize the pivotal role of these approaches in optimizing the reaction pathways and enhancing the catalytic performance. Additionally, by employing machine learning to elucidate and validate the CO_2 reduction mechanisms, we aim to predict previously unexplored reduction pathways and intermediates, thereby providing a robust theoretical and technical foundation for the tailored production of advanced chemicals in industrial applications.

2 Single-atom catalysts: design, preparation, characterization and prediction

2.1 Formation and optimization of single-atom catalysts

The preparation of SACs involves dispersing isolated metal atoms onto a stable support to prevent aggregation into larger clusters or nanoparticles.[37] Single-atom dispersion requires strong metal–support interactions to prevent aggregation during synthesis or post-synthesis processes.[38,39] In wet-chemical methods, aggregation is inevitable unless the metal atoms or complexes strongly bind to the support. SACs consist of isolated metal atomic sites dispersed on a support, where metal atoms are not arranged in continuous lattice structures as in metal nanoparticles, nor embedded in the surface lattice of metal oxides or other non-oxide compounds. These active sites typically consist of the metal atom and its first coordination shell, composed of oxygen or other non-metallic atoms. The active sites interact with nearby surface structures, such as metal atoms and oxygen vacancies. These sites adsorb and activate reactant molecules, forming surface intermediates, and ultimately generate products. The structural complexity of SACs arises from the diversity of the ligand shells surrounding the dispersed metal atoms. These metal atoms are often located at defect sites on the support, such as step edges, corners, and voids. Although the metal atoms are isolated, their chemical and coordination environments vary significantly depending on their specific positions. This variation in ligand coordination induces different electronic perturbations in the metal atoms' valence orbitals, altering their electronic structure and ultimately affecting the catalytic performance (Fig. 1). Furthermore, the addition of two or more metal atoms to a single dispersed metal atom can form dimers or trimers, which often exhibit distinct an sometimes enhanced catalytic properties.

Yizheng Li

Mr Yizheng LI is a PhD candidate, who is jointly affiliated with the Hong Kong Polytechnic University and the Eastern Institute of Technology (Ningbo) and advised by Prof. Zhangxing CHEN and Prof. Jinyue YAN. He received his M.Eng. and B.Eng. from China University of Petroleum-Beijing. His research interests primarily include interpretable artificial intelligence, machine learning, petroleum engineering, building energy management, clean energy production, energy policy, and sustainable engineering education.

Qidong Li

Mr Qidong Li earned his Master's degree in Electrical Engineering through a joint program between the University of British Columbia and the National Research Council Canada, after graduating with a Bachelor's degree in Process Equipment and Control Engineering from China University of Petroleum-Beijing. His research focuses on battery thermal management systems.

CO_2RR has attracted considerable attention in recent years, especially in the fields of photocatalysis, electrocatalysis, and Fischer–Tropsch synthesis (FTS).[40,41] SACs have gained prominence due to their exceptional catalytic properties. When supported on materials such as carbon-based substrates, SACs can mimic the activation and reduction capabilities of homogeneous catalysts, facilitating CO_2 conversion into small organic molecules.[42] Despite their potential, challenges persist, including the strong C═O bond dissociation energy, competition with the hydrogen evolution reaction (HER), low product selectivity, and catalyst stability issues.[43] Recent advancements have focused on optimizing SACs to enhance CO_2 activation, tune electronic properties, and improve reaction pathways. For example, supporting SACs on nitrogen-doped carbon materials has been shown to significantly improve the CO_2RR efficiency by enhancing the charge transfer and stabilizing the key intermediates. Understanding and controlling the metal–support interaction is critical for improving the SACs performance, as it modulates the CO_2 binding energy and the formation of the desired products.

The use of a single-atom iron catalyst supported on carbon nitride has been demonstrated, where metal sites dispersed on a nitrogen-doped carbon matrix serve as active centers for the adsorption and activation of CO_2,[44] enabling its reduction to CO and hydrocarbons. Similarly, ultra-thin nitrogen-doped carbon nanosheets have been employed as supports for single-atom nickel catalysts, significantly enhancing the efficiency of CO_2RR. By integrating principles from homogeneous catalysis with quantum computational chemistry, these SACs have been engineered to mimic the CO_2 activation processes observed in homogeneous systems. Co-doping with carbon and nitrogen further boosts the catalytic efficiency by modifying the electronic environment of the SACs, optimizing the CO_2 adsorption, and facilitating the formation of reaction intermediates.

To further enhance the SACs catalytic performance, future development should focus on the following key aspects:

1. Optimization of metal–support interactions: tuning the interactions between metal active sites and the support is essential for improving the SACs performance. By modifying these interactions, the electronic structure of the metal atoms can be adjusted, thereby improving the CO_2 adsorption and facilitating the formation of reaction intermediates.

2. Synergistic effect of multi-metallic sites: incorporating two or more metal atoms into SACs can enhance its catalytic performance. This synergistic effect provides new avenues for SACs optimization.

3. Regulation of surface defects: introducing specific defects, such as oxygen vacancies or nitrogen doping, can effectively modulate the electronic environment of SACs, optimizing the catalytic pathways and enhancing the catalytic efficiency and selectivity.

4. Catalyst stability and reusability: improving the stability of SACs and preventing the loss or aggregation of metal atoms during prolonged reactions is essential for the industrial application of SACs.

2.2 Performance predictions by DFT and machine learning

2.2.1 Structure-determined catalytic properties of single-atom catalysts. The structure of SACs is crucial for their catalytic properties, particularly in CO_2RR. The geometric and electronic characteristics of SACs govern their activity, selectivity, and stability across different reaction conditions.[45] These properties depend on the active metal center,[46,47] its coordination environment, promoters, and support materials. Geometric features such as coordination number, bond lengths, and bond angles influence the distribution of active sites and the catalyst's interaction with reaction intermediates.[45–48] Catalysts

Yuxuan Yi

Mr Yuxuan Yi is currently pursuing a Master's degree in Environmental Engineering at the National University of Singapore. His undergraduate research at Dalian University of Technology focused on photocatalysis. Presently, his research interests encompass seawater reverse osmosis and environmental data analytics.

Lifen Liu

Lifen Liu is currently a Full Professor in the School of Chemical Engineering, Marine and Life Science, Dalian University of Technology. She received her Bachelor, Master and Ph.D. degrees from DUT. She was a Visiting Scholar and Collaborator at the Sydney University, Australia from 1997–1999, a Research Associate at HKUST, HK, and a Senior Research Fellow at the Georgia Institute of Technology, USA (2010.10–2011.05). Her current and main scientific interests include environmental nanotechnology and pollution control engineering, specifically single-atom catalysts, functional electrode and fuel cell technologies for cost-effective processes. She has published more than 200 international peer-reviewed papers.

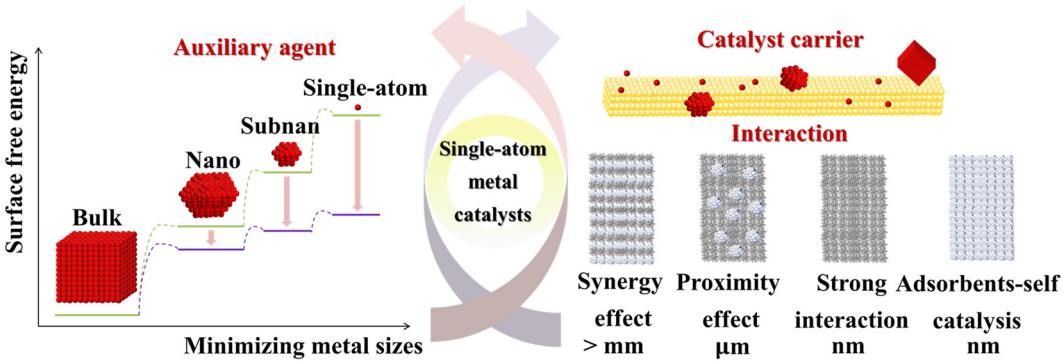

Fig. 1 Effects of metal-size reduction on the surface free energy of auxiliary agents, and the interactions between auxiliary agents and catalyst supports in single-atom catalysts.

with unsaturated coordination sites often exhibit higher activity due to the better adsorption of the intermediates, and the bond structure affects CO_2 activation by modulating the electronic interactions between the catalyst and adsorbates.

The electronic structure of SACs is linked to bonding between the metal centers and reactants, with key factors such as the d-band center, electronegativity, and ionization energy playing a crucial role. The position of the d-band center controls electron transfer to adsorbed species, enhancing CO_2RR.[49] Electronegativity and ionization energy govern the catalyst's ability to donate or withdraw electrons, affecting interactions with CO_2 and products. Promoters such as alkali metals can further modify the electronic structure, adjusting the electron density and enhancing the adsorption of intermediates. The support material affects the metal dispersion, catalyst stability, and geometric configuration, influencing the electronic interactions and CO_2RR efficiency.

ML models are increasingly used to predict SAC performance in CO_2RR, leveraging high-dimensional data to uncover structure–activity relationships. Parameters such as the coordination number, bond length, d-band center, and electronegativity are key input features in these models. Computational methods like DFT predict the binding and adsorption energies, which are essential for understanding the CO_2RR mechanisms. These properties are fundamental in the rational design of optimized catalysts.[50]

Key structural features vary for different CO_2RR pathways, including photocatalysis, electrocatalysis, and thermocatalysis (Table 1). In photocatalysis, the band gap and electronic affinity govern light absorption and electron transfer efficiency. Electrocatalysis emphasizes charge transfer and the d-band center for efficient electron flow at the electrode surface. In thermocatalysis, geometric descriptors like the coordination number and bond lengths are critical for the reaction rate and product distribution, particularly at high temperatures.

2.2.2 Explanation and validation of the reaction mechanism. The use of SACs for CO_2RR to produce value-added chemicals, through photocatalysis,[51] electrocatalysis,[27] and thermocatalysis,[52] requires an in-depth understanding of the underlying reaction mechanisms. Recent developments in ML, integrated with DFT, have become pivotal tools for unraveling these mechanisms by predicting the reaction dynamics, energy profiles, and intermediates, thus advancing the design of efficient catalysts.

Machine learning models, particularly those integrated with DFT calculations, have shown significant potential in predicting the electronic structure and energetics of SACs. For instance, the first-coordination sphere–support interaction (FCSSI) has emerged as a key descriptor for regulating the catalyst performance in CO_2RR. ML models, such as extreme gradient boosting regression (XGBR), utilize DFT-derived data to predict limiting potentials (UL), which directly influence reaction pathways and selectivity toward specific products.[53] Moreover, ML has proven effective in identifying intermediate species and elucidating reaction pathways. For example, the use of ML models to predict product selectivity in SACs supported on modified graphene (*e.g.*, MoO_4 on H-doped graphene and FeO_4 on N,O-doped graphene) demonstrated the ability to distinguish between products like formate and CO.[54] This highlights the potential of ML to identify SACs that minimize side reactions, such as HER,[55] and favor target products such as formic acid or CO. In addition to predicting known pathways, ML models can uncover previously unobserved reaction mechanisms. For example, the prediction of new C–C coupling processes in graphdiyne-based SACs for C_3 product formation offers new possibilities for CO_2RR, potentially enhancing the overall CO_2 conversion efficiency.[56] These models provide an integrated framework to validate existing hypotheses and predict novel catalytic routes, which is critical for developing more selective and efficient CO_2RR catalysts.

The application of graph neural networks (GNNs) and transformer-based models, such as CatBERTa, has further strengthened the predictive capabilities of ML models. These hybrid models can predict adsorption energies by utilizing spatial coordinates and textual representations of catalytic systems, thus allowing for the discovery of unknown intermediates and reaction pathways.[57] Additionally, ML models can identify optimal reaction conditions, such as metal centers (Mn, Co, Ru, Os) and support interactions, which are crucial for product

Table 1 Summary of the descriptors for machine learning models of single-atom catalysts in CO_2 reduction reactions *via* photocatalysis, electrocatalysis, and thermocatalysis

Descriptors	Photocatalysis	Electrocatalysis	Thermocatalysis
Structural and geometrical properties			
Bond lengths	✓	✓	✓
Bond angles	✓	✓	✓
Atomic radius	✓	✓	✓
Coordination numbers	✓	✓	✓
Atomic positions (one-hot encoding)	✓	✓	✓
Number of specific element atoms	✓	✓	✓
Surface hollow, bridge, and top sites	✓	✓	✓
Chemical and elemental properties			
Electronegativity	✓	✓	✓
Ionization energy	✓	✓	✓
Atomic mass	✓	✓	✓
d-electron count	✓	✓	✓
d-band center	✓	✓	✓
Valence electron number	✓	✓	✓
Electron affinity	✓	✓	✓
Physics-informed descriptors			
SOAP (smooth overlap of atomic positions)	✓	✓	✓
MBTR (many-body tensor representation)	✓	✓	✓
ACSF (atom-centered symmetry functions)	✓	✓	✓
Synthesis and experimental parameters			
Calcination temperature (°C)		✓	✓
Calcination time (h)		✓	✓
Reduction temperature (°C)		✓	✓
Reduction time (hours)		✓	✓
Reaction temperature (°C)	✓	✓	✓
Reaction pressure (MPa)	✓	✓	✓
GHSV	✓	✓	✓
Time on stream (h)	✓	✓	✓
Experimental data and metrics			
Tafel slope (η)		✓	
Band gap (eV)	✓		
Catalyst per volume (mg mL^{-1})	✓		
Sacrificial agent	✓		

selectivity, as seen in the case of CH_4 production.[58] By integrating ML with computational studies, the exploration of CO_2RR mechanisms becomes more systematic and accurate. This approach not only allows for the identification of new intermediates and reaction steps, but also enables experimental validation, which accelerates the discovery of high-performance SACs. The synergy between ML predictions and experimental data fosters an iterative process that refines reaction mechanism models, facilitating the rational design of SACs for efficient CO_2RR.

ML-based methods, when coupled with quantum-level simulations, offer valuable insights into CO_2RR mechanisms on SACs. These approaches facilitate the prediction of intermediates, reaction pathways, and optimal conditions, leading to the design of SACs with tailored properties for enhanced CO_2RR performance.

2.2.3 Designing single-atom catalysts and optimizing reaction conditions. The design and optimization of SACs for CO_2RR rely on predicting catalytic properties, which depend on the catalyst structure, support material, and reaction conditions. ML models are highly effective in predicting the impact of the synthesis strategies on catalyst performance by using descriptors, such as the coordination number, d-band center, and local chemical environments. These models aid in selecting the most efficient SAC compositions and predicting the adsorption energies of CO_2RR intermediates, thereby guiding the design of SACs for specific products, such as CO or formic acid.[59] Additionally, ML assists in optimizing reaction conditions (*e.g.*, temperature, pressure, and electrolyte composition), which are crucial for enhancing the catalyst stability, selectivity, and efficiency. Through DL and active learning, ML can identify the reaction conditions that suppress side reactions, such as hydrogen evolution.[60]

Active ML methods, including reinforcement and self-supervised learning, enable models to autonomously search for optimal SAC structures and reaction conditions. These models iteratively refine predictions through continuous feedback from experimental data, accelerating the discovery of high-performance SACs. Moreover, ML facilitates the design of catalyst supports and surface modifications by considering local coordination environments and the electronic effects induced by dopants.[54] In practical applications, ML has already contributed to the discovery of SACs such as Zn-NP_3 and Sn-P_4, which exhibit promising CO_2RR activity and selectivity.[60] By predicting the optimal catalyst structures and conditions before synthesis, these models minimize trial-and-error processes and accelerate the development of efficient SACs for CO_2RR. Furthermore, ML-driven frameworks enable

the high-throughput screening of catalyst materials and reaction parameters, expediting the discovery of novel SACs. The iterative refinement of SAC structures and reaction conditions continuously enhances the catalyst performance and CO_2 utilization strategies.

In summary, integrating ML with SAC design and optimization offers a transformative approach to developing high-performance catalysts. By predicting the optimal catalyst structures and reaction conditions, ML accelerates the discovery and optimization of SACs for more efficient CO_2RR.

2.2.4 Mutual verification framework integrating DFT and machine learning. DFT plays a pivotal role in elucidating the electronic structure, adsorption behavior, and reaction mechanisms at active sites, effectively complementing experimental studies. With its high accuracy, DFT facilitates the interpretation of experimental observations and the prediction of catalytic performance, effectively bridging experimental data with theoretical models. These calculations are indispensable for optimizing the design of SACs and refining catalytic pathways. However, the high computational cost of DFT poses challenges, particularly when modeling large or complex systems.

To address these computational limitations, various ML models, including Random Forest (RF), Support Vector Machines (SVM), Neural Networks (NN), and Graph Neural Networks (GNNs), have been employed to predict the catalytic performance of SACs and gain insights into their underlying mechanisms. These models utilize the structural and electronic properties of catalysts to predict the catalytic activity, stability, selectivity, and key reaction parameters such as activation energy and charge transfer.

From a mechanistic perspective, Zhu *et al.*[61] identified eight key descriptors that characterize the electronic and structural properties of catalysts: N_d (the number of d-shell valence electrons of metal atoms), which influences reactivity; EA (electron affinity), representing the metal's ability to accept electrons; CT (charge transfer from metal-zeolites to intermediates), quantifying electron redistribution during the catalytic step; H_c (hydrogen count in carbon atoms) and H_s (hydrogen in H_2O, CH_3OH, CH_4), which influence the reactant activation; N_c (coordination number of carbon to metal), capturing the interaction strength between the carbon-based intermediates and the metal; P_s (number of proton/electron transfers), offering insights into the proton or electron transfer mechanisms; and N_{HB} (hydrogen bonds), which stabilize the reaction intermediates.

To predict CT (e)—the charge transfer between the metal-zeolites and intermediates—ML models are trained using three key features: C (coordination number for intermediate to metal), N_o (coordination number for oxygen to metal), and NI (number of atoms in intermediates). These features capture the strength of the interaction between intermediates and the metal, the interaction of oxygen-containing species with the metal, and the complexity of the intermediates. By analyzing the relationships between these features and charge transfer, ML models help identify active sites and understand the critical electronic redistributions necessary for catalytic activity (Fig. 2).

Once trained, ML models can predict key DFT-derived quantities, such as CT (e), activation barriers, and intermediate energies, at a significantly reduced computational cost. This accelerates the screening of catalysts and intermediates, allowing DFT calculations to focus on the most promising candidates. Additionally, ML enables efficient exploration of complex parameter spaces, uncovering insights into the reaction mechanisms that DFT alone might not fully resolve.

From a mechanistic perspective, ML provides deeper insights into catalytic processes by identifying key descriptors and elucidating their influence on reactivity. It offers a fundamental understanding of how electronic structures drive charge transfer and how intermediate coordination impacts catalytic efficiency. The integration of ML with DFT and experimental data accelerates SACs discovery and optimization, providing a powerful framework for designing next-generation catalytic materials with tailored properties.

2.3 Efficient and innovative methods for the preparation of single-atom catalysts

The preparation methods for SACs impact their performance in CO_2 reduction, with each method offering distinct advantages and limitations (Fig. 3). Co-precipitation is cost-effective and scalable, yielding SACs with high surface area and catalytic activity.[62] However, high metal loading can cause aggregation, reducing catalyst efficiency. It is suitable for large-scale production, but struggles with metal dispersion at high loadings.[63]

Ion exchange enables precise metal deposition, increasing active site density and surface area,[64,65] but suffers from high reagent consumption and catalyst instability[66] due to site degradation.[67] Chemical vapor deposition (CVD) and atomic layer deposition (ALD) achieve atomic-level metal dispersion, yet remain cost-intensive and complex, limiting their scalability. The sol–gel method, though solvent-free with good dispersion, risks metal aggregation at high temperatures. Electrodeposition, often following substrate cleaning and electropolishing, facilitates nanostructure formation, while spin-coating efficiently deposits functional layers like perovskites, followed by annealing. Hydrothermal synthesis grows metal oxide nanowires, and photolithography with etching fabricates precise substrate patterns.[68]

For large-scale applications, co-precipitation offers cost efficiency and scalability, whereas CVD and ALD provide superior atomic precision but face economic and scalability constraints. The optimal method depends on balancing the cost, precision, and industrial feasibility.

2.4 Comparison in the characterization of single-atom catalysts

Accurate characterization is crucial for understanding the structure–property relationships of SACs, which exhibit unique catalytic behaviors due to their atomically dispersed active sites. The complexity of SACs, including their coordination environment, electronic structure, and metal–support interactions, requires the use of complementary techniques that

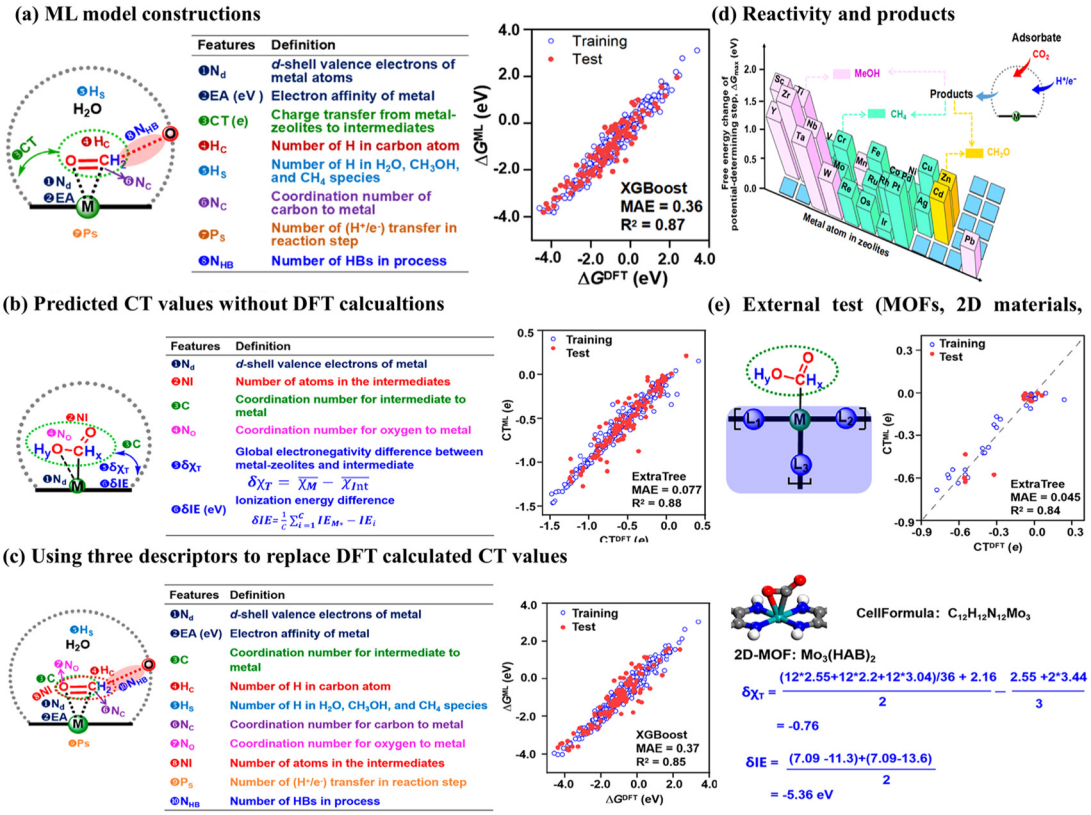

Fig. 2 Application of DFT and machine learning/deep learning in predicting reaction pathways (a) Machine learning model with eight features, and the ability the XGBoost algorithm in predicting the free energy change in CO_2 reduction process, (b) Machine learning model with six features for CT prediction on metal-zeolites, (c) 10-feature scheme, using three additional descriptors to replace the CT values, for free energy change prediction in the CO_2 reduction process using XGBoost, (d) flow chart of reactivity and product calculation of CO_2 reduction reactions on 26 metal-zeolites, (e) external test in the CO_2 reduction process using ExtraTree. Reproduced from ref. 61, with permission of ACS Catalyst, copyright 2022.

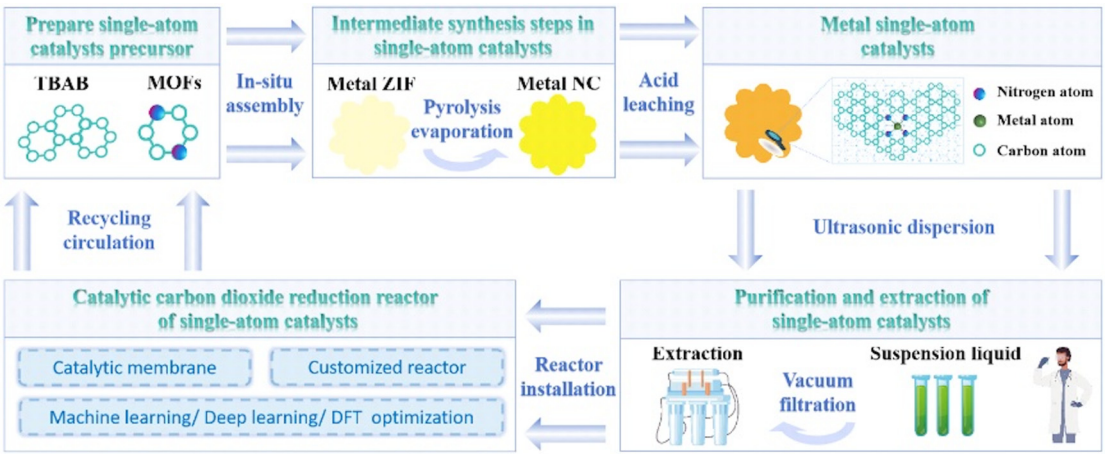

Fig. 3 Synthesis, purification, and application of single-atom catalysts for CO_2 reduction: from precursor preparation to catalytic reactor implementation.

each address specific aspects of their structure and performance.

Microscopic methods, such as transmission electron microscopy (TEM) and scanning transmission electron microscopy (STEM) combined with energy-dispersive X-ray spectroscopy (EDS), provide spatial insights into the dispersion and localization of single atoms. TEM reveals the distribution of active sites, while STEM-EDS achieves atomic-scale resolu-

tion, providing detailed insights into the elemental composition and structural features. Spectroscopic techniques, including X-ray absorption fine structure (XAFS) and X-ray photoelectron spectroscopy (XPS), play a crucial role in probing the local coordination environment, oxidation state, and chemical bonding of single atoms. These methods reveal the critical interactions between the active sites and the support, while also characterizing the surface's elemental composition and chemical states.

In situ techniques, such as Fourier transform infrared spectroscopy (FTIR) and Raman spectroscopy, allow for real-time monitoring of active sites and surface chemical environments during reactions. FTIR monitors the adsorption behavior and vibrational modes of reaction intermediates, while Raman spectroscopy tracks dynamic changes in catalytic sites under reaction conditions, elucidating the reaction mechanisms. Thermal characterization methods, such as temperature-programmed reduction (TPR) and thermogravimetric analysis (TGA), assess metal–support interaction strength, reducibility, and thermal stability, all of which are essential for evaluating the catalyst durability under operational conditions.

The integration of these techniques offers a comprehensive understanding of SACs, connecting their atomic structure, electronic properties, and reaction mechanisms to the catalytic performance and selectivity. This holistic approach not only advances fundamental knowledge, but also informs the rational design of next-generation catalysts for CO_2 hydrogenation and other critical reactions.

3 Photocatalytic CO_2 reduction

3.1 Mechanism of photocatalytic reduction

The photocatalytic reduction of CO_2 with H_2 utilizes light energy, typically from ultraviolet or visible light, to drive the reaction, converting CO_2 and H_2 into valuable products such as methane, methanol, and other organic compounds. This process involves several critical steps. First, photon absorption occurs when the semiconductor catalyst absorbs light, exciting electrons from the valence band to the conduction band, thereby generating electron–hole pairs (e^-/H^+). The electrons and holes are then separated and migrate within the catalyst's conduction and valence bands, with electrons (e^-) participating in the CO_2RR, while holes (H^+) are involved in the oxidation of H_2. During CO_2RR, the electrons reduce CO_2 into products such as carbon monoxide, methanol, or methane, depending on the catalyst and reaction conditions. This reaction proceeds through e^- and H^+ transfer, with different intermediates forming based on the targeted product. The oxidation process involves H^+ at the catalyst surface, which oxidize H_2, generating H^+ that provide the protons necessary for CO_2RR. These key steps are crucial for optimizing the catalyst performance and guiding the development of efficient photocatalysts for CO_2 hydrogenation (Table 2).

In photocatalytic CO_2 hydrogenation, the use of SACs is particularly effective. SACs, with their atomic-level dispersion on supports, create well-defined active sites that facilitate efficient electron and proton transfer, thereby optimizing the reduction steps. These catalysts enhance the reaction rates, selectivity, and stability by minimizing energy barriers, stabilizing reaction intermediates, and promoting specific electron transfer processes. The preparation of SACs—including metal choice, support material, and synthesis method—significantly influences their catalytic performance. By fine-tuning the electronic properties of metal atoms and their interaction with the support, SACs can be optimized to enhance CO_2 activation, improve product selectivity, and boost the overall efficiency of the photocatalytic reduction process (Fig. 4).

Inspired by photosynthesis, photocatalysis leverages light-driven redox reactions for CO_2 fixation. In this process, photogenerated charge carriers are separated in the semiconductor[69] and transferred to the catalyst surface, where they react with adsorbed CO_2. This results in the conversion of CO_2 into valuable organic compounds such as formic acid, CO, alcohols, and hydrocarbons.[70] Compared to traditional CO_2 purification methods, photocatalysis offers advantages such as mild reaction conditions, low energy consumption, and minimal environmental impact, positioning it as a promising technology for sustainable CO_2 utilization and carbon management.[71]

3.2 Reaction kinetics of photocatalytic reduction

The reaction kinetics of photocatalytic CO_2RR, particularly when catalyzed by SACs, begins with photon absorption, which excites electrons and generates active sites on the cata-

Table 2 Equilibrium potential (E_{eq} *vs.* RHE) and reaction enthalpy (ΔH) for the reduction of CO_2 to different products

Product	CO_2 reduction pathways	E_{eq} (V)	ΔH (kJ mol^{-1})
CO	$CO_2 + 2e^- + 2H^+ \rightarrow CO + H_2O$	−0.10	−41.2
CH_4	$CO_2 + 8e^- + 8H^+ \rightarrow CH_4 + 2H_2O$	0.17	−253.0
C_2H_6	$2CO_2 + 14e^- + 14H^+ \rightarrow C_2H_6 + 4H_2O$	0.14	264.3
C_3H_8	$3CO_2 + 20e^- + 20H^+ \rightarrow C_3H_8 + 6H_2O$	0.09	374.2
C_2H_4	$2CO_2 + 12e^- + 12H^+ \rightarrow C_2H_4 + 4H_2O$	0.08	127.8
CH_3OH	$CO_2 + 6e^- + 6H^+ \rightarrow CH_3OH + H_2O$	0.03	−131.0
C_2H_5OH	$2CO_2 + 12e^- + 12H^+ \rightarrow C_2H_5OH + 3H_2O$	0.09	216.1
C_3H_7OH	$3CO_2 + 18e^- + 18H^+ \rightarrow C_3H_7OH + 5H_2O$	0.1	331.2
CH_3CHO	$2CO_2 + 10e^- + 10H^+ \rightarrow CH_3CHO + 3H_2O$	0.06	130.1
HCOOH	$CO_2 + 2e^- + 2H^+ \rightarrow HCOOH$	−0.12	−31.2
CH_3COOH	$2CO_2 + 10e^- + 10H^+ \rightarrow CH_3COOH + 2H_2O$	0.11	122.1

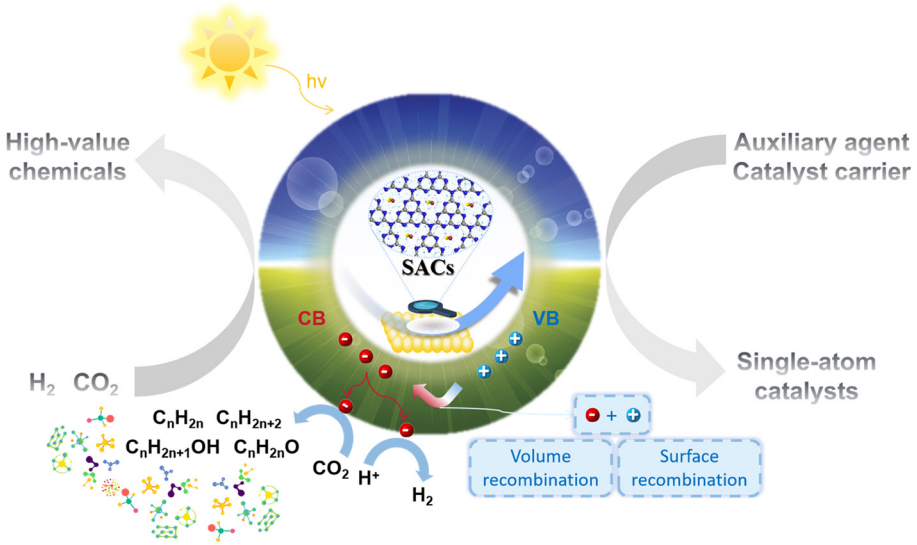

Fig. 4 Engineering single-atom catalysts for efficient photocatalytic CO_2 reduction: modulation of the electron pair alignment and recombination dynamics using auxiliary agents and catalyst supports to enhance the catalyst stability.

lyst surface. The efficiency of this process is largely influenced by the metal's ability to facilitate electron transfer and the support material's role in stabilizing the excited states. Early research on photocatalytic CO_2RR dates back to the 1970s, initially focusing on semiconductor materials for water splitting applications. In the 1980s, research shifted towards using solar energy to drive CO_2RR into organic chemicals, with early studies concentrating on methane and carbon monoxide production. Initial reaction models were oversimplified, typically assuming surface adsorption and electron transfer as the primary steps. However, with advancements in the catalyst materials and reaction conditions, the kinetics of the process became increasingly complex, involving multiple steps, various intermediates, and charge carrier participation.

As catalyst materials diversified, selectivity and product distribution in photocatalytic CO_2RR emerged as critical research themes. Different catalysts not only affect the separation efficiency of electron–hole pairs, but also play a decisive role in the formation pathways of intermediates, thus determining the final product. The reaction kinetics of photocatalysis involve several complex stages, including catalyst excitation, electron–hole pair separation and migration, and the formation and transformation of intermediates.

Enhancements in reaction kinetics are often achieved through orbital coupling between metal atoms and adjacent ligands, especially in bimetallic sites. For instance, Pt–Ru dimers on g-C_3N_4 demonstrate significantly improved catalytic performance for CO_2RR and HER by weakening the binding strength with intermediates and adjusting the orbital energy levels.[72] This strategy allows for more efficient catalytic processes by optimizing the interaction between the catalyst and the reaction intermediates.

$$r_{PC} = k_{PC} \cdot I_{light}^{n_{PC}} \cdot (C_{CO_2})^{a_{PC}} \cdot (C_{H_2})^{b_{PC}}$$

The rate of a photocatalytic reaction (r_{PC}) is generally linearly dependent on the light intensity (I_{light}). However, under high light conditions, the reaction rate may become limited by the catalyst's electron carrier capacity, resulting in kinetic saturation. The rate is also influenced by the concentrations of CO_2 (C_{CO_2}) and H_2 (C_{H_2}), as well as by the surface adsorption characteristics of the catalyst, illumination conditions, and reactant concentrations (*e.g.*, n_{PC}, a_{PC}, b_{PC}). Moreover, the lifetime of the photogenerated electrons and the efficiency of the charge carrier separation are critical factors that impact the overall reaction efficiency. The separation efficiency of charge carriers is closely related to the catalyst surface structure and the light intensity. If photogenerated electrons recombine with holes on the catalyst surface, the reaction efficiency will be significantly reduced. Therefore, optimizing the charge carrier migration and separation efficiency is crucial for improving the performance of photocatalytic CO_2 reduction.

3.3 Photocatalytic reduction of CO_2 using single-atom catalysts

3.3.1 Mechanisms of auxiliary agents in photocatalysts. The photocatalytic reduction of CO_2, first explored by Fujishima *et al.*[73] in 1972 using TiO_2 for water splitting and later advanced by Halmann[74] in 1978 for CO_2 conversion to formic acid and methanol, has attracted substantial interest due to its potential in sustainable CO_2 utilization. This process offers several advantages, including mild reaction conditions (ambient temperature and pressure), the use of renewable solar energy, and an environmentally friendly approach.[75] However, the efficiency of photocatalytic CO_2RR is still hindered by challenges such as inefficient charge separation,[76] low energy transfer efficiency, and limited CO_2 adsorption and activation on catalyst surfaces. Addressing these limitations is crucial for advancing practical applications.[77,78]

Optimizing CO_2 adsorption and activation on the catalyst surface is key to improving the photocatalytic performance. However, a detailed understanding of surface site dynamics is still lacking. Feng *et al.*[79] introduced an innovative strategy by constructing Mn single-atom sites on TiO_2 nanostructures, which modified the local coordination environment, enhancing CO_2 adsorption and the localization of photogenerated electrons, thus improving the catalytic efficiency. Similarly, Zhang *et al.*[80] developed a dual-site system combining Au/Co double-monoatom-supported CdS for CO_2RR. In this system, Co sites promote CO_2 adsorption and reduction, while Au sites facilitate the collection of photogenerated electrons, selectively producing CO and CH_4 with 82% selectivity. This design underscores the importance of effectively distributing photogenerated charges across different single-atom sites to enhance the photocatalytic selectivity.

Auxiliary agents play a vital role in optimizing SACs for photocatalytic CO_2RR by modulating their electronic structures, stabilizing active sites, and facilitating charge transfer. Strategies such as defect engineering, heteroatom doping, and co-catalyst integration significantly influence reaction pathways, improving the catalytic activity and product selectivity.[81–83] One effective approach involves introducing oxygen vacancies or structural distortions in the catalyst support to enhance the CO_2 adsorption and charge separation. For instance, in Pd-SA/TiO_2, oxygen vacancies created under a hydrogen-rich atmosphere serve as strong anchoring sites for Pd single atoms, preventing agglomeration and tuning their electronic structure. This modification increases the CO selectivity to 92.51% and catalytic activity to 56.84 μmol g^{-1} h^{-1} by facilitating charge transfer and minimizing electron–hole recombination.[84]

Heteroatom doping further refines the electronic properties of SACs by modifying charge distribution at the active sites. Doping with elements such as nitrogen, sulfur, or phosphorus stabilizes the reaction intermediates and enhances CO_2 activation. In Cu-based SACs, nitrogen-doped carbon supports strengthen metal–support interactions, promoting C–C coupling and enabling selective C_{2+} product formation. The dopant atoms shift the d-band center of the Cu sites, reducing the activation energy barriers and optimizing multi-electron transfer processes.[85]

Co-catalyst incorporation provides another effective strategy for improving SACs performance by introducing additional charge transfer pathways or cooperative catalytic mechanisms.[86] Overall, the integration of defect engineering, heteroatom doping, and co-catalysts significantly enhances SACs performance in photocatalytic CO_2RR. These strategies collectively improve charge transfer, stabilize reaction intermediates, and suppress recombination losses, leading to higher catalytic efficiency and selectivity.

3.3.2 Supports for photocatalysts. The inherent chemical inertness of CO_2, combined with weak adsorption and high activation barriers, poses significant challenges for efficient CO_2RR, especially at low concentrations. Additionally, competitive HER further hinders progress in this area. To overcome these obstacles, Lyu *et al.*[87] designed oxygen-deficient Co_3O_4 hollow nanoparticles supported on a macroporous N-doped carbon framework. The introduction of oxygen vacancies disrupted the Co–O–Co symmetry, enhancing CO_2 adsorption and activation, while the macroporous structure increased active site availability and facilitated the transport of photogenerated electrons. This work underscores the importance of active site symmetry modulation for improving catalytic performance in low-concentration CO_2RR.

MOFs have attracted considerable interest for their ability to modulate electron transport in photocatalysis, owing to their tunable porosity, high surface area, and the potential to tailor active sites. Porphyrins and their derivatives, known for their excellent photosensitivity, can create conductive pathways through their stacked units. The incorporation of metals further enhances electron transport, although precise control of these pathways remains a challenge. Huang *et al.*[88] employed a thermal-induced strategy, using thorium ions as unstable coordination nodes in porphyrin-based MOFs to control electron transport, thereby improving carrier separation and enhancing photocatalytic efficiency. This study provides valuable insights into carrier dynamics within photocatalytic systems. MOFs provide high surface area, tunable porosity, and defined coordination sites, ensuring uniform metal dispersion and electronic modulation. Their confinement effect prevents metal aggregation, while enhancing CO_2 activation. MOF-derived carbons retain structural integrity and improve conductivity, facilitating charge transfer and reaction kinetics.

Recent developments in SACs have demonstrated their potential for CO_2RR, driven by their unique electronic properties, high dispersion, and enhanced catalytic activity through defect engineering. SACs offer additional active sites at the atomic scale, which significantly enhance catalytic performance. Cheng *et al.*[89] utilized the large surface area and planar conjugate structure of g-C_3N_4 to anchor Ni single atoms through a self-limiting method.[90] This approach not only stabilized the Ni single atoms, but also promoted efficient CO_2 adsorption and electron transfer from g-C_3N_4 to Ni *via* Ni–N coordination, resulting in a CO_2 conversion rate that is 7.8 times higher than that of pure g-C_3N_4 under visible light. This highlights the critical role of tuning active sites for improving CO_2RR efficiency.[91]

Zhang *et al.*[92] developed Co-SA@SP by anchoring single-atom cobalt on commercial superconducting carbon black. The Co–N_4 coordination sites in this material reduced the $CO^{\bullet}$ desorption energy barrier, enhancing the catalytic reactivity, CO selectivity (84.2%), and stability under UV light. The suppression of HER further promoted CO_2RR, demonstrating the potential of SACs to inhibit competitive reactions and enhance selectivity. This simple and cost-effective catalyst offers a promising pathway for scalable photocatalytic CO_2RR in industrial applications. Catalyst carriers critically influence SACs' photocatalytic CO_2RR by modulating the electronic structure, charge transfer, and active site stability. The carrier dictates metal–support interactions, adsorption strength, and reaction selectivity.

Semiconductor supports with oxygen vacancies effectively anchor single metal atoms, preventing aggregation while tuning their electronic environment. In Pd-SA/TiO_2, oxygen vacancies enhance metal–support interactions, optimizing Pd's oxidation state and CO_2 activation. This defect engineering improves the charge separation and suppresses recombination, boosting the catalytic efficiency.[84]

Carbon-based supports, such as graphene, CNTs, and nitrogen-doped carbon (N–C), offer high conductivity and π-conjugation networks that enhance charge transport. In Cu-SACs, N–C stabilizes Cu atoms, improving C–C coupling and favoring C_{2+} products. Strong metal–support interactions (SMSI) optimize Cu's electronic state, lowering activation barriers and increasing the CO_2 conversion selectivity.[85] Hybrid architectures incorporating plasmonic nanostructures or co-catalysts further enhance the SACs performance. Plasmonic-metal-SACs hybrids use localized surface plasmon resonance (LSPR) to extend the carrier lifetimes and improve charge transfer, lowering the activation barriers. Co-catalyst integration facilitates charge separation and directional electron flow, optimizing the reaction selectivity.[86]

In summary, defect engineering, conductivity tuning, and confinement effects are key to improving the SACs stability and reactivity. Future research should focus on optimizing the metal–support interactions and charge transfer pathways to enhance SAC-based CO_2RR.

3.3.3 Perovskite-structured photocatalysts. In photocatalytic CO_2RR, perovskite-based SACs have garnered considerable attention due to their unique structural and electronic properties, which enhance their catalytic performance. Perovskite materials, with their distinctive crystal structures, offer multiple advantages in the context of SACs for CO_2RR.

The perovskite structure, characterized by a corner-sharing octahedral arrangement of metal cations and halide anions, provides a versatile platform for modulating the electronic properties, optimizing the charge carrier dynamics, and facilitating enhanced photocatalytic activity. In $Cs_3Sb_{0.5}Bi_{1.5}Cl_4Br_5$ perovskite catalysts, the formation of a built-in electric field (IEF) within heterojunctions facilitates efficient electron–hole separation, a key factor in improving the photocatalytic CO_2RR efficiency. The coupling of these materials with other catalysts, such as Bi-BTC frameworks, has shown that the synergistic effects between the two components can significantly boost photocatalytic performance, leading to high CO and CH_4 yields.[93]

In addition, engineering the electronic structure of perovskites through doping or phase transition can further enhance their catalytic properties. For example, doping perovskite structures with metal ions or using phase transitions to generate piezoelectricity can increase the adsorption capacity for CO_2 and reduce the energy barrier for its conversion.[94] The piezoelectric effect, induced by phase transition under external stimuli, can produce a polarized electric field that accelerates CO_2 activation, contributing to improved catalytic efficiency. In the case of $Cs_3Bi_2Br_9$-based perovskites, the introduction of Cu atoms into the perovskite lattice has been shown to promote charge separation and enhance the electronic structure of the material, which further lowers the energy barriers for CO_2RR. The atomically dispersed Cu acts as a critical site for charge transfer, improving the selectivity for CO production while maintaining stability over multiple cycles.[95]

The engineering of heterojunctions by combining perovskites with other semiconductors, such as Co_3O_4, has proven highly effective for promoting efficient charge separation. The formation of built-in electric fields at the heterojunction interface enhances the photocatalytic CO_2RR performance, with Na-ion incorporation further strengthening these electric fields to boost CO_2 adsorption and activation.[96] Thus, perovskite SACs possess unique properties, such as their tunable band structures, efficient charge separation, and enhanced CO_2 adsorption, all of which play crucial roles in improving the directional selectivity of photocatalytic CO_2RR.[97] These structural features, coupled with innovative doping strategies and heterojunction formation, position perovskite-based SACs as promising candidates for the efficient conversion of CO_2 into valuable chemicals (Fig. 5).

4 Electrocatalytic CO_2 reduction

4.1 Mechanism of electrocatalytic reduction

CO_2RR converts electrical energy into chemical energy, producing valuable small molecules *via* electrochemical reduction.[92] However, in aqueous systems, the HER often competes with CO_2RR, significantly reducing selectivity and efficiency. To address this, the development of highly efficient electrocatalysts with high activity, selectivity, and stability is crucial for advancing CO_2RR technology. SACs have emerged as promising candidates due to their well-defined active sites, maximizing atom utilization. The performance of SACs is primarily determined by the electronic structure and coordination environment of the single metal atoms, which can effectively modulate CO_2 adsorption, activation, and reduction. SACs promote the reduction process by facilitating the formation of key intermediates such as $^*CO_2$, $^*COOH$, and $^*CHO$ through unique reaction pathways, while minimizing HER by optimizing the binding energies of hydrogen and CO_2 intermediates. The enhanced selectivity and efficiency of SACs arise from the atomic-level control over the reaction mechanisms, enabling precise tuning of the product distribution. Ongoing efforts to improve SACs for CO_2RR have focused on stabilizing the metal sites, increasing conductivity, and optimizing the local electronic environment to achieve scalable, practical performance.

CO_2RR is a complex multi-electron, multi-proton process where intermediates like $^*CO$ are crucial for C_2 product formation. Strong interactions between $^*CO$ and metal catalysts (*e.g.*, Pt, Fe, Ni) can poison the active sites, favoring HER and diminishing the CO_2RR efficiency.[98] On the other hand, metals with weak $^*CO$ binding (*e.g.*, Au, Ag, Zn) facilitate $^*CO$ desorption, which prevents efficient C–C coupling and results in CO as the final product.[99] However, metals with moderate $^*CO$ binding strengths, such as Cu, Ni, Co, and Zn, are among

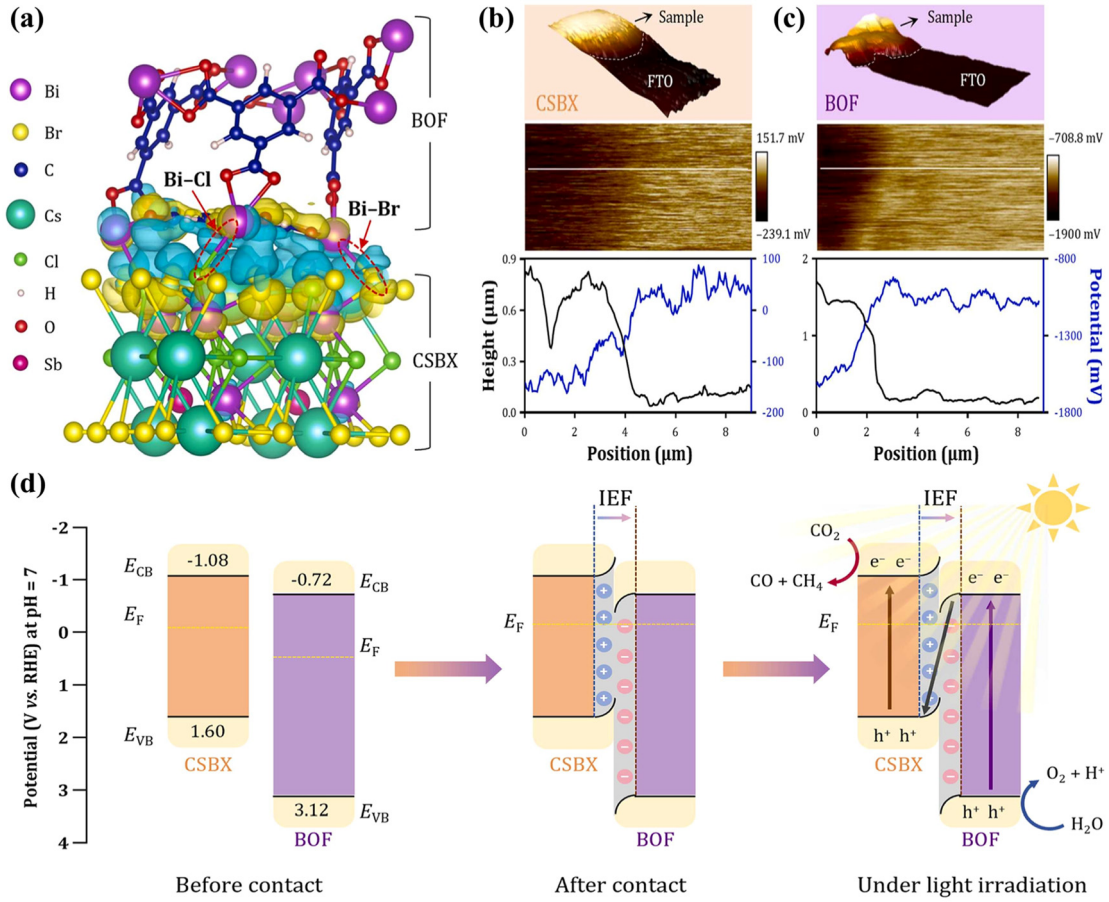

Fig. 5 Lead-free halide-perovskite-based heterojunction: (a) charge density difference (isosurface level, 0.04 e Å^{-3}) over the CSBX/BOF heterojunction. The yellow and cyan regions represent the positive and negative electron density isosurfaces, respectively, KPFM surface potential images (middle), and the corresponding topography and surface potential line profiles (bottom) for (b) CSBX and (c) BOF three-dimensional topographical maps (top). (d) Schematic of the band structures of CSBX and BOF (left), interfacial charge transfer and the formation of an IEF upon hybridisation (middle), and CSBX/BOF S-scheme heterojunction under light irradiation (right). Reproduced from ref. 93, with permission of *Applied Catalysis B: Environment and Energy*, copyright 2025.

the few catalysts capable of selectively producing C_2 and other organic carbon products,[100] striking a balance between $^*CO$ binding and desorption, thereby enabling effective C–C coupling.

Electrocatalytic CO_2RR typically occurs in an electrochemical cell, where an electrode (a metal or alloy electrode) catalyzes the reaction between CO_2 and H_2, converting them into useful chemicals. During this process, CO_2 is adsorbed onto the catalyst surface, where it is activated through electron transfer, generating reactive intermediates like $^*CO_2^{\bullet-}$ (a radical anion) or $^*CO_2H$ (a hydrogenated intermediate). This step requires overcoming the adsorption energy barrier between CO_2 and the electrode, typically occurring on metal electrodes (*e.g.*, copper, silver, gold). The reduction reaction involves the transfer of electrons and protons; electrons are delivered *via* the electrode, while protons come from the electrolyte. The electrode surface reduces CO_2 intermediates, generating species such as $CO_2^{\bullet-}$ or CO_2H.

The electrocatalytic reaction proceeds through the formation of intermediates, which are progressively reduced to final products like methanol, methane, and other hydrocarbons (Fig. 6). The overpotential, defined by the current density and voltage applied, plays a critical role in determining the product selectivity. Different electrocatalysts significantly affect the distribution of products. For instance, copper-based catalysts are often superior to others, promoting a range of carbon-containing organic products such as alkanes, alkenes, and alcohols, while silver and gold catalysts typically favor the formation of CO.

Thus, understanding and optimizing the interaction between CO_2 intermediates, the electronic properties of the metal catalysts, and reaction conditions are key to enhancing the efficiency and selectivity of electrocatalytic CO_2RR.

4.2 Reaction kinetics of electrocatalytic reduction

In recent years, significant progress has been made in understanding the electrocatalytic CO_2RR using SACs, leading to improved catalytic performance. SACs are particularly appealing due to their high metal atom utilization, distinct electronic properties, and excellent catalytic efficiency. However, the isolated active sites in SACs can limit their effectiveness in reac-

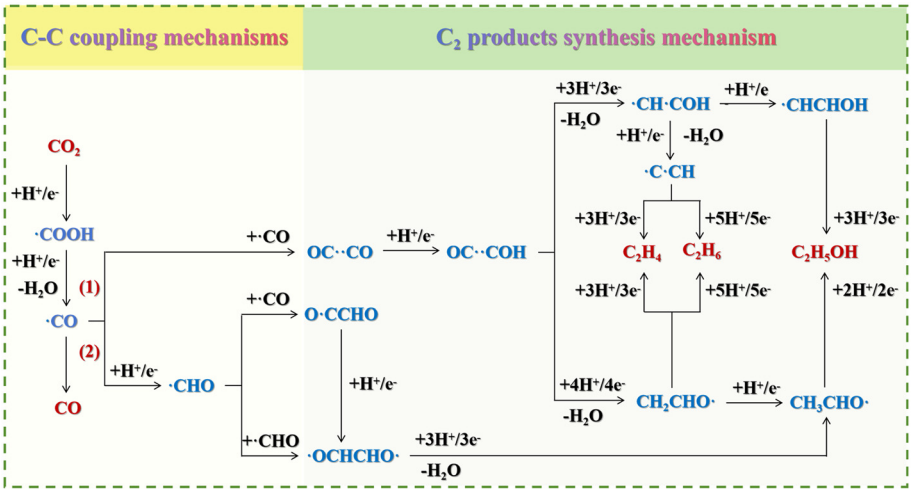

Fig. 6 Reaction pathways of CO_2 reduction to produce value-added C_2 chemicals (C_2H_4, C_2H_6, and C_2H_5OH) *via* electrocatalysis by adding (1) $^*CO$ before H^+/e^- and (2) H^+/e^- before $^*CO$.

tions that require the simultaneous activation of multiple reactants or intermediates. To address this limitation, strategies have been developed to combine the advantages of SACs with multi-atomic sites, resulting in "fully exposed metal cluster catalysts" (FECCs).[101] These FECCs can simultaneously activate different reactants, enhancing the reaction kinetics and improving the overall electrocatalytic performance.

Recent studies[102] have demonstrated that tuning the atomic dispersion of metal species within SACs can significantly enhance the catalytic efficiency. For instance, by adjusting the pyrolysis temperature, researchers have successfully transitioned nickel (Ni) species from clusters to single-atom scales, resulting in a Ni FECC with superior CO_2RR performance. The optimized Ni FECC achieved a FE of up to 99% for CO production, with a CO partial current density of 347.2 mA cm^{-2}, and exhibited stable performance over 20 hours of electrolysis. Theoretical calculations revealed that sulfur doping plays a crucial role in regulating the charge distribution across multiple Ni sites, thus accelerating the reaction kinetics and facilitating efficient CO_2RR to CO.

Another study[103] focused on the development of a model Ni SAC with well-defined Ni–N_4 coordination on a conductive carbon support, which was used to explore the CO_2RR mechanism. Using advanced operando techniques, such as X-ray absorption spectroscopy, Raman spectroscopy, and near-ambient XPS, it was found that the Ni^+ sites in the Ni SAC were highly active for CO_2 activation, acting as the actual catalytic sites for the CO_2RR. Electrochemical kinetics studies identified the rate-determining step of the CO_2RR as the conversion of $^*CO_2$@ + H^+ → $^*COOH$, providing key insights into the mechanistic details of CO_2RR.

Despite the outstanding performance of SACs in CO_2RR, the relationship between their electronic and geometric structures and their electrocatalytic properties remains an area of ongoing investigation. Factors such as the coordination environment of metal atoms, the nature of the conductive support, and the interactions with secondary catalysts all significantly influence the efficiency and selectivity of SACs in CO_2RR. Understanding these structure–function correlations is critical for the rational design of SACs that exhibit high activity, selectivity, and stability.[104]

The kinetics of electrocatalytic CO_2RR are influenced by several key factors, including current density, applied voltage, catalyst surface properties, and the concentrations of CO_2 and H_2. Typically, the reaction rate is proportional to the current density (j, A cm^{-2}), with the reaction rate increasing as the current density increases, until a saturation point is reached. The overpotential (η) represents the difference between the required voltage for the reaction and the theoretical voltage, reflecting the activation barrier on the catalyst surface and significantly affecting the reaction rate. This relationship is often described by the Tafel equation, which characterizes the logarithmic dependence of the reaction rate on the overpotential:

$$\eta = a_{EC} + b_{EC} \cdot \log j$$

Additionally, the reaction rate (r_{EC}) is affected by the concentrations of CO_2 and H_2. The rate for CO_2RR typically follows the equation:

$$r_{EC} = k \cdot j$$

$$r_{EC} = k_{EC} \cdot (C_{CO_2})^{a_{EC}} \cdot (C_{H_2})^{b_{EC}}$$

where C_{CO_2} and C_{H_2} represent the concentrations of CO_2 and H_2, and a_{EC} and b_{EC} are the reaction orders with respect to CO_2 and H_2, and typically determined experimentally.

Overall, SACs have demonstrated remarkable potential in CO_2RR, with atomically dispersed active sites, tunable electronic structures, and enhanced reaction kinetics. However, challenges remain in the catalyst design, synthesis, and characterization. Future research should focus on developing novel synthetic strategies to precisely control the atomic dispersion, improving the catalyst stability under practical con-

ditions, and further elucidating the structure–activity relationships.

4.3 Electrocatalytic reduction of CO_2 using single-atom catalysts

4.3.1 Influence of auxiliary agents on electrocatalytic performance. SACs offer exceptional activity, selectivity, and atom efficiency, making them highly suitable for selective CO_2RR.[105] The performance of SACs is largely governed by the morphology and coordination environment of the metal center, typically in M–N–C structures.[106] These structures facilitate the adsorption and activation of CO_2, as well as the reduction process, by enabling precise control over the binding energies of key intermediates, such as $^*CO_2$, $^*COOH$, and $^*CHO$. One example is the Ni–N/NCNT catalyst developed by Kim *et al.*,[107] which achieved a FE of 96.73% for CO production in a zero-gap CO_2 electrolyzer with an optimized membrane electrode assembly (MEA). The asymmetrical Ni–N–C structure enhances CO_2 adsorption, facilitates high CO coverage, and suppresses HER, improving the CO_2 electroreduction activity by boosting metal utilization and CO_2RR efficiency.[108] In contrast, Yang *et al.*[109] demonstrated that halogen activation of metal sites can further enhance performance. Bromide, in particular, promotes the selective exposure of planar bismuth surfaces, resulting in a high current density and greater than 90% selectivity for formic acid, whereas chlorides and iodides tend to disorganize the active sites.[110]

The CO_2RR involves complex intermediates and competing reaction pathways, making optimization challenging. Jin *et al.*[111] addressed this by constructing atomically dispersed heterodiatomic pairs, where $^*COOH$ intermediates bridge across heteroatomic sites, lowering their formation energy. This modification enhances electron delocalization *via* Mo–Fe d–d orbital coupling, which promotes $^*CO$ desorption and improves CO selectivity. The introduction of dual- and multi-active centers has also gained attention for its ability to activate multiple reactants, improving selectivity and product diversity. For CO_2RR, dual-site catalysts often feature separate sites for CO_2 activation and subsequent hydrogenation or C–C coupling. The spatial arrangement of these sites influences the migration of intermediates, and optimizing $^*H$ coverage can help mitigate HER, improving the selectivity for CO_2RR over hydrogen evolution.

Single-atom alloy catalysts (SAAs) are another promising approach for CO_2RR to C_{2+} products, although challenges remain in achieving selective C–C coupling. Cao *et al.*[112] reported on a Bi–Cu SAA catalyst that achieved 73.4% FE for C_{2+} products. The interaction between Bi and Cu modulated the electronic structure of Cu, lowering the CO_2 adsorption and activation energy, enhancing intermediate formation, and improving the C_{2+} selectivity. This study highlights the potential of SAAs in regulating active sites, and provides a new strategy for catalyst design. In a different approach, Cai *et al.*[113] used Pd atoms for CO_2RR to formic acid with a Pd/C–Pt/C composite electrode, demonstrating a new method for low-temperature aqueous-phase electrocatalysis. Additionally, Quan *et al.*[114] developed nitrogen-coordinated Cu SACs (Cu/NC) for CO_2 electrocarboxylation with styrene, achieving 92% FE and nearly 100% product selectivity for phenylsuccinic acid.

Metals such as Fe, Co, Cu, Zn, and Sn are increasingly used in CO_2RR due to their distinct product selectivity. Sn, In, and Pb primarily produce formic acid while effectively inhibiting HER,[115,116] whereas Zn, Au, and Ag favor CO production due to their strong interaction with the CO^* intermediate, which is crucial for large-scale CO production.[117–119] However, the high cost of Au and Ag limits their practical application. Cu, as the only metal capable of producing C_{2+} products, holds significant potential, as C_2 products (ethanol and ethylene) offer greater commercial value compared to C_1 products (CO and methane).[120] Despite this, the structural sensitivity of copper single atoms and their role in CC coupling remain areas of ongoing research. It has been assumed that CO_2RR to both CO and C_2 products occurs at the same Cu site, but recent studies suggest that distinct Cu sites may be involved in these steps.[121] Further mechanistic investigations are required to clarify these processes and optimize the catalyst performance. Cu-based catalysts have been extensively studied for CO_2RR, with various modifications improving their selectivity and efficiency. This strategy can be extended to other Lewis-acid metals to further enhance the CO_2RR performance. Wang *et al.*[122] developed an InBi bimetallic catalyst supported on In_2O_3 nanodots on $Bi_2O_2CO_3$ nanosheets, where the synergistic effect between the metals and the enhanced CO_2 adsorption led to 97.17% FE in an H-type electrolyzer.

Heteroatom doping, particularly with nitrogen, sulfur, or phosphorus, alters the electronic properties of the support material and enhances the SACs activity. Nitrogen-doped carbon supports improve the interaction between metal centers and CO_2, facilitating CO_2 adsorption and reduction. This doping stabilizes the metal sites and prevents agglomeration, thus improving the catalyst's stability over prolonged reactions. The coordination environment of the metal center is further optimized by the inclusion of multiple heteroatoms in the support structure. In Cu SACs, nitrogen-doped carbon support adjusts the binding strength of $^*CO$ and $^*COOH$ intermediates, enhancing CO_2RR to C_2H_4. This synergy between the metal and support is crucial for maximizing the CO_2RR performance. Co-catalysts, often in the form of small nanoparticles or sub-nanoclusters, have been integrated with SACs to promote cooperative catalysis. In these tandem systems, one site activates CO_2, while the other facilitates CO coupling, leading to higher-order products such as C_2H_4 and CH_4. Cu SACs coupled with copper nanoclusters exhibit enhanced selectivity for C_{2+} products by promoting CO_2RR to CO, followed by coupling at the NP site.[123]

Moreover, modifying the coordination environment around the metal site further enhances the SACs performance. For instance, Cu SACs supported by N_2-bidentate sites in a graphdiyne structure show higher selectivity for methane production, with reduced side reactions. This design achieves a FE of 80.6% for methane and a current density of 160 mA cm^{-2}.[124]

The support curvature also affects the SACs activity. Ni SACs supported on spherical carbon materials exhibit optimized nanocurvatures, which influences the interfacial electric field, modulating intermediate adsorption during CO_2RR. This results in a CO partial current density of 400 mA cm^{-2} at 99% FE.[125]

Cu SACs supported by nitrogen-doped carbon quantum dots (CQDs) exhibit enhanced catalytic performance, with a FE of over 80% for ethanol production and stable performance over 50 hours. This improvement stems from the atomic dispersion of Cu sites and the interaction with the nitrogen-doped support.[126]

4.3.2 Electrocatalyst support materials. In 2023, Cui *et al.*[127] designed an Al–Cu tandem catalyst supported on carbon nanotubes (CNTs) to improve CH_4 production *via* efficient CO_2RR and enhanced electron transfer, significantly boosting the CH_4 selectivity. This catalyst system uses the complementary properties of Al and Cu, facilitating the conversion of CO_2 and increasing the overall efficiency of methane production. Similarly, Ding *et al.*[128] developed a cascade catalyst combining SnS_2 nanosheets with single-atom Sn, achieving 82.5% ethanol selectivity. In this system, CO_2 is first reduced to formic acid on SnS_2, followed by bicarbonate formation at the single-atom Sn sites, where C–C coupling occurs *in situ* to yield ethanol. This mechanism exemplifies the synergy between different catalytic sites and materials, promoting high selectivity for desired products.

While precious metals such as Ru, Pd, and Pt have demonstrated high efficiency in CO_2RR, their high cost and limited scalability prompt the exploration of more affordable and scalable SACs.[129–131] Liu *et al.*[132] developed a Sn–Cu diatomic catalyst by introducing Sn into isolated Cu sites, which achieved a FE of 99.1% for CO production.[133] The high efficiency of this catalyst is attributed to its efficient atom utilization, SMSI, and the high unsaturation of the coordination environment around the metal atoms. Additionally, the nitrogen-doped porous carbon support improves mass transfer, ensuring that the catalyst can maintain high performance over extended periods.

Su *et al.*[134] reported a Cu/Zn hierarchical porous catalyst that inhibits HER, while favoring alcohol formation. This catalyst enhances intermediate interactions with the surface. Furthermore, it features a porous structure that increases the density of surface active sites and improves the surface-to-volume ratio, promoting the formation of C_2 products. In another study, Chen *et al.*[135] employed a Cu^{2+} electrolyte to balance Cu ion dissolution and deposition, achieving 83.3% ethylene selectivity after 4 hours of electrolysis.[136] The periodic removal of accumulated bicarbonate during the reaction further stabilized the catalyst, maintaining high performance and selectivity. The combination of ultrafast thermal shock synthesis and pore engineering enhanced the electrode's reactive surface area, facilitated charge transfer, and improved selectivity, ultimately boosting the catalyst's overall efficiency. Fan *et al.*[137] addressed stability concerns in acidic systems by modifying the electrode surface with benzimidazole-functionalized ionomer groups. This modification activated CO_2 and enhanced C–C coupling, achieving over 80% multi-carbon selectivity. The control of the microscopic water environment and the improvement of the catalyst stability under acidic conditions further contributed to the high performance.

Oxygen or nitrogen vacancies in the support material can improve metal–support interactions and increase the number of available active sites. Supports like TiO_2 or carbon materials with oxygen vacancies can stabilize metal sites and facilitate electron transfer, lowering the activation energy for CO_2RR. This enhances the reaction rates and improves selectivity for valuable products such as C_{2+} compounds. Using $Ti_3C_2O_2$-based MXene supports showed that the asymmetric coordination of the metal center improved CO_2RR and product selectivity. The support's ability to modulate the metal's electronic properties and interaction with intermediates contributed to enhanced catalytic activity, such as improved formic acid production.[138]

The chemical composition of the carrier is also important. Nitrogen-doped carbon supports, for instance, can enhance the electronic environment of SACs, improving CO_2 adsorption and the formation of C_{2+} products. Supports with high surface area and tunable porosity, such as MOFs, are ideal for dispersing metal atoms uniformly, improving accessibility to reactants and boosting the catalyst efficiency.[139]

Tandem catalysis, where SACs are combined with nanoclusters or sub-nanometric catalysts, can further enhance performance. These hybrid systems allow for cooperative interactions, where one component activates CO_2 and the other facilitates CO coupling to form higher-order products. Cu-based SACs combined with copper nanoclusters show improved selectivity for C_{2+} products due to this synergy.[123] The stability of SACs is also influenced by the support. Conductive and stable supports, like graphene or carbon nanotubes, help maintain the high dispersion of metal atoms and ensure efficient electron transfer, preventing aggregation and preserving catalytic activity. A study of CuFONC, a carbon composite with Cu single atoms supported by F, O, and N-doped motifs, found that the carrier stabilized the Cu sites, enhancing CO–C coupling and selectivity for C_2 products. The carrier's chemical environment strengthened the interaction between Cu and CO intermediates, leading to an FE of 80.5%.[140] The curvature of the carrier also plays a role. Ni SACs on spherical carbon exhibited superior CO_2 reduction performance due to the stronger electric fields generated by the nanocurvature. These fields help optimize the adsorption of intermediates, enhancing the SACs activity.[125]

Overall, these studies demonstrate the effectiveness of SACs in CO_2RR, highlighting various strategies for improving the efficiency, selectivity, and stability. The use of different metal combinations, such as Cu–Sn, Cu–Bi, and Cu–Zn, as well as modifications to support structures and electrolyte conditions, plays a critical role in tailoring the catalytic properties and enhancing the overall CO_2RR. The transition to more affordable, scalable SACs is essential for advancing CO_2RR technologies, with significant potential for commercial applications in producing valuable carbon-based products.[141]

4.3.3 Graphene-structured electrocatalysts. Graphene-based SACs offer significant advantages for CO_2RR due to their excellent electronic conductivity, high surface area, and the ability to fine-tune the local electronic environment of active sites. The key to enhancing the catalytic activity of graphene-based SACs lies in the design of graphene's structure, particularly through defect engineering, heteroatom doping, and the creation of 3D graphene (3DGr) architectures. The 3D structure of graphene not only prevents issues such as re-stacking observed in 2D graphene, but also improves mass and electron transport, essential for efficient CO_2RR. The introduction of defects and heteroatoms (*e.g.*, nitrogen, sulfur) in the graphene matrix further modifies the electronic properties of the catalyst, enabling better activation of CO_2 and stabilization of the reaction intermediates.

The modification of the graphene matrix plays a critical role in improving the selectivity and efficiency of CO_2RR. For example, nitrogen doping and the introduction of vacancy defects have been shown to modulate the electronic environment, optimizing the charge distribution at the active sites. In iron-based SACs supported on nitrogen-doped graphene (Fe–N–C), nitrogen plays a key role in lowering the CO_2RR onset potential and widening the potential range for achieving high CO FE. This is due to the enhanced charge capacity of the *COOH intermediate, which facilitates selective CO_2RR over competing reactions like hydrogen evolution. Additionally, the introduction of defects provides additional catalytic sites, improving reactivity while maintaining the material's structural integrity (Fig. 7).[142,143]

Another significant aspect of graphene-based SACs is the tailored design of the interfacial microenvironment (Fig. 7). For instance, in CoPc catalysts supported on a graphitic carbon nitride/graphene (C_3N_4/G) matrix, the graphene matrix enriches CO_2 and dissociates H_2O to produce active hydrogen species, further enhancing the catalytic performance. The interaction between C_3N_4 and graphene also optimizes the electronic properties of the active sites, leading to a higher turnover frequency (TOF) and exceptional CO selectivity, with a FE consistently above 98%.[144] These findings highlight the importance of both structural and compositional engineering in graphene-based SACs, demonstrating that the manipulation of defects, doping, and microenvironment tuning are essential for improving the CO_2RR performance.

Thus, the combination of hierarchical graphene structures, defects, heteroatom doping, and interfacial microenvironment design results in SACs with enhanced catalytic stability, product selectivity, and CO_2RR efficiency. These strategies are crucial for advancing the development of efficient and high-performance catalysts for CO_2 conversion.

5 Thermocatalytic CO_2 reduction based on Fischer–Tropsch synthesis

5.1 Reaction kinetics and mechanism of Fischer–Tropsch synthesis

The FTS mechanism for CO_2 hydrogenation on SACs involves several key stages: adsorption of CO_2, activation *via* hydrogenation, and product formation through well-defined pathways. The reaction starts with the adsorption of CO_2, which is then hydrogenated to form active intermediates such as *CO, methanol, or methane. This process typically follows a surface adsorption–reaction–desorption cycle. Temperature plays a crucial role in these reactions; FTS generally occurs at elevated temperatures (300–500 °C), where the reaction heavily relies on thermal energy to overcome activation barriers. CO_2 hydrogenation to olefins and other FTS products is an exothermic reaction, with low temperatures favoring product formation, while higher temperatures enhance the reaction kinetics. In practice, unreacted syngas is often recycled to optimize conversion. High pressure conditions also favor olefin formation. The reaction equations of CO_2 hydrogenation to alkane, olefin and alcohol are shown in the following formulas:

$$CO_2 + H_2 \leftrightarrow CO + H_2O$$

$$CO + 2H_2 \rightarrow \frac{1}{n}C_nH_{2n} + H_2O$$

$$CO + \frac{2n+1}{n}H_2 \rightarrow \frac{1}{n}C_nH_{2n+2} + H_2O$$

$$CO + 2H_2 \rightarrow \frac{1}{n}C_nH_{(2n+1)}OH + \frac{n-1}{n}H_2O$$

The reaction rates in FTS follow the Arrhenius equation, where the rate is exponentially dependent on temperature:

$$r_{FTS} = A \cdot e^{-\frac{E_a}{RT}}$$

Here, r_{FTS} is the reaction rate, A is the pre-exponential factor, E_a is the activation energy, R is the gas constant, and T is the absolute temperature. The reaction rate also depends on the concentrations of CO_2 and H_2, with the dependence often described by a power-law expression:

$$r_{FTS} = k_{FTS} \cdot (C_{CO_2})^{a_{FTS}} \cdot (C_{H_2})^{b_{FTS}}$$

$$r_{FTS} = k_{FTS} \cdot (C_{CO_2})^{a_{FTS}} \cdot (C_{H_2})^{b_{FTS}} \cdot e^{-\frac{E_a}{RT}}$$

where k_{FTS} is the rate constant, and a_{FTS} and b_{FTS} are the reaction orders with respect to CO_2 and H_2, respectively. Higher reactant concentrations typically increase the reaction rate, particularly at elevated temperatures.

At lower temperatures, the reaction is often limited by electron transfer and hydrogenation steps. At higher temperatures, the rate is more influenced by the activation energy. Temperature adjustments allow for selective production of the desired products: lower temperatures favor methane, while higher temperatures promote olefin and alcohol formation.

The reaction mechanism varies depending on the catalyst and temperature. For Fe-based catalysts, the active phase has shifted from metallic iron to the FeC_x phase in recent studies,[145] following the Mars-van Krevelen (MvK) mechanism. This mechanism divides the reaction into the surface and outer layers of the catalyst, with fast reactions following the Langmuir–Hinshelwood (L–H) pathway, where most of the FTS activity occurs at a small fraction of active sites. The slow

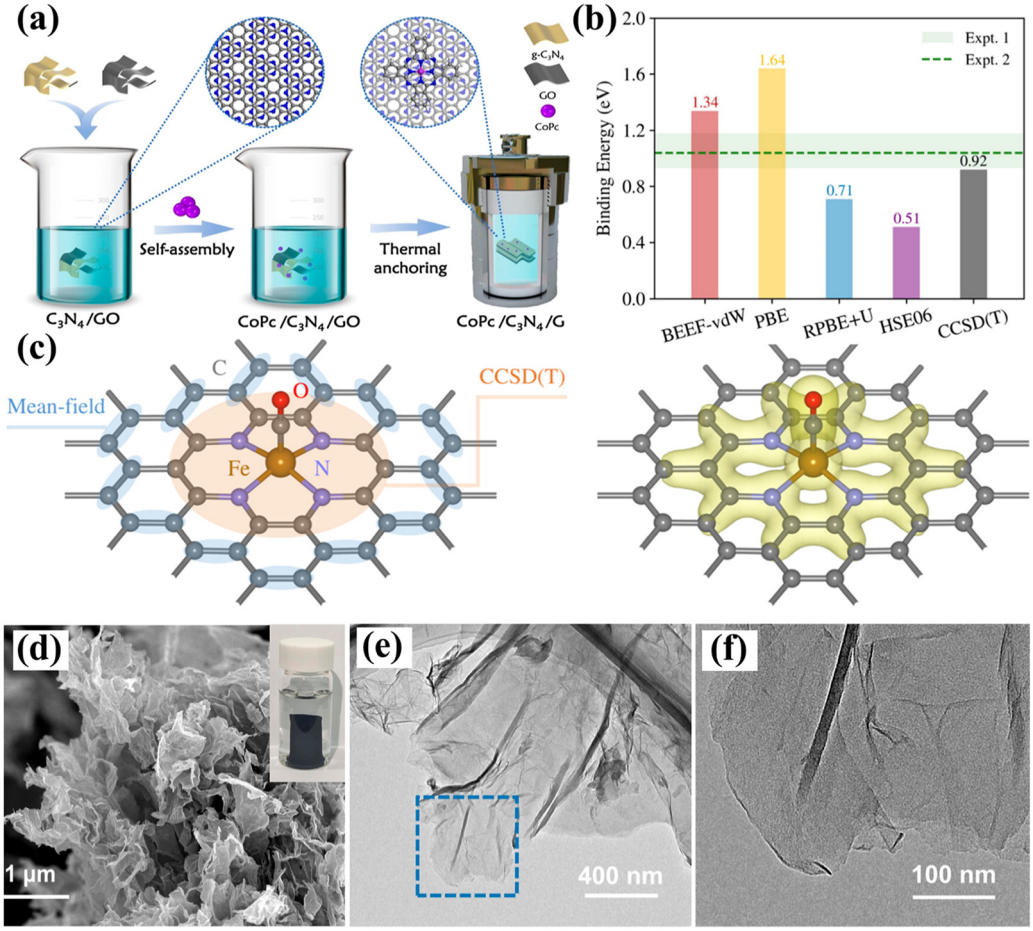

Fig. 7 Illustration and benchmark of the local embedding for modeling single-atom catalysts, along with the synthesis procedure and morphology characterization: (a) schematic of the synthesis process of $CoPc/C_3N_4/G$,[142] (b) binding energies of CO on FeN_4 predicted using DFT with four functionals (BEEF-vdW, PBE, RPBE+U, and HSE06) and CCSD (T) local embedding. Experimental TPD measurements of the CO binding energy are 0.93–1.18 eV and 1.04 eV,[143] (c) schematic showing fragment selection in local embedding calculations (left) and electron density of the FeN_4C_{10}-embedded fragment (right), (d–f) SEM, TEM, and HR-TEM images of $CoPc/C_3N_4/G$.[143] Reproduced from ref. 142 and 143, with permission of ACS Catalysis, copyright 2024.

pathway, governed by the MvK mechanism, occurs predominantly at the majority of active sites.[146]

Brübach *et al.*[147] explored the kinetics of CO_2 hydrogenation over Fe-based catalysts, identifying key inhibitory factors such as the strong adsorption of oxygen-containing species and the effects of shifting the equilibrium to lower CO partial pressures. They proposed new kinetic expressions based on the L–H model, which incorporate these dynamics.

$$r_{\mathrm{RWGS}} \approx \frac{k_{\mathrm{RWGS}}\left(p_{\mathrm{H_2}}^{0.5}p_{\mathrm{CO_2}} - \dfrac{p_{\mathrm{CO}}p_{\mathrm{H_2O}}}{K_{\mathrm{eq}}p_{\mathrm{H_2}}^{0.5}}\right)}{\left(1 + a_{\mathrm{RWGS}}\dfrac{p_{\mathrm{H_2O}}}{p_{\mathrm{H_2}}}\right)^2}$$

$$r_{\mathrm{FT}} \approx \frac{k_{\mathrm{FT}}p_{\mathrm{CO}}p_{\mathrm{H_2}}}{\left(1 + a_{\mathrm{FT}}\dfrac{p_{\mathrm{H_2O}}}{p_{\mathrm{H_2}}} + p_{\mathrm{CO}}b_{\mathrm{FT}}\right)^2}$$

Product distribution in CO_2 hydrogenation typically follows the Anderson–Schulz–Flory (ASF) model:

$$W_n = n(1+\alpha)^2\alpha^{n-1}$$

where n is the carbon number, W_n is the mass fraction of hydrocarbons with n carbon atoms, and α is the chain growth probability.

The integration of reaction kinetics models with ML and DL is an emerging direction for uncovering unknown mechanisms. Sun *et al.*[148] employed a combined approach of artificial neural networks (ANN) and response surface methodology (RSM) to simulate the product distribution of FTS in a microchannel reactor. The model demonstrated the ability to predict the formation rates of hydrocarbon products in the C_2–C_{15} range, as well as the olefin-to-paraffin ratio (OPR), showing advantages in rapid convergence and high predictive accuracy. This approach offers a novel perspective for studying the kinetics of complex catalytic processes. Wang *et al.*[149] developed a radial basis function neural network (RBFNN), which offers fast convergence and reduced computation time, to generate

data matrices with a limited set of experimental data. A comprehensive kinetic model, coupled with a genetic algorithm (CKGA), was used to select mechanisms and infer potential reaction pathways. The RSM-based RBFNN, constructed *via* central composite design, processed responses and subsequent singular/multiple optimizations to produce the data matrix. This approach provides a highly practical and valuable tool for process engineering design and practice, especially for understanding product distribution during FTS (Fig. 8).

5.2 Single-atom catalysts in CO_2 conversion *via* Fischer–Tropsch synthesis

The synthesis of SACs for CO_2 hydrogenation typically involves the reduction of metal precursors to isolated metal atoms, which are subsequently dispersed onto supports through thermal or chemical reduction. The catalytic performance of SACs is strongly influenced by strong metal–support interactions (SMSI), which stabilize metal atoms and facilitate the activation of CO_2 and H_2. These interactions play a crucial role in determining the reaction pathway and product selectivity. Notably, the metal's d-band structure modulates the adsorption and activation of CO, ultimately affecting the product distribution. For instance, Co_1/W_6S_8 favors the formation of C_{2+} hydrocarbons,[150] whereas Ni_1/W_6S_8 exhibits higher selectivity toward methanol, highlighting the critical role of metal–support interactions in controlling the reactivity and selectivity.

Iron-based SACs, particularly those supported on CeO_2, further exemplify the influence of support interactions and preparation conditions on catalytic performance. Wang *et al.*[151] demonstrated that iron species can be effectively dispersed on CeO_2 *via* the deposition–precipitation method, forming $Fe^{\delta+}$ single atoms under CO_2 hydrogenation conditions (300 °C, 2 MPa). These single atoms are stabilized through Fe–O–Ce bonds, which play a key role in CO_2 activation. Additionally, co-doping with Ru enhances the iron dispersion and prevents metal aggregation under reaction conditions, thereby stabilizing the catalyst and modulating the electronic environment of the active sites.

The CO_2 hydrogenation reaction on SACs proceeds through the adsorption of CO_2 and H_2 onto metal atoms, leading to protonation and electron transfer, forming intermediates such as $^*CO$ and $^*HCOOH$. The binding strength of CO_2 and its intermediates is a critical factor in determining the reaction mechanism and product distribution. Metal–support interactions, particularly those involving reducible oxides such as CeO_2, facilitate electron transfer and optimize the binding energies of the reaction intermediates, thereby influencing the catalytic selectivity.

In conclusion, the rational design of SACs for CO_2 hydrogenation necessitates precise control over metal dispersion,

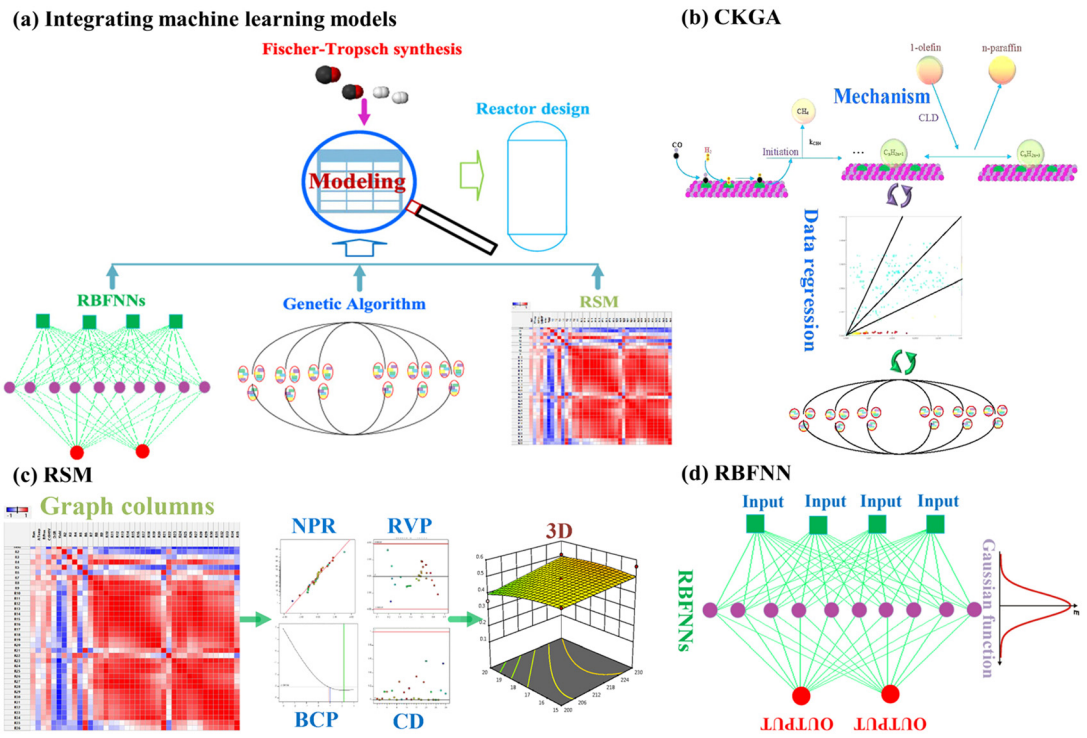

Fig. 8 Machine learning assists in unveiling the reaction kinetics process: (a) integrating machine learning models, (b) schematic of the genetic algorithm (GA) for mechanism discrimination and data regression (CLD refers to chain-length dependent), (c) schematic of RSM for significance analysis (NPR refers to a normal plot of residues, RVP refers to residues *versus* predictions, BCP refers to the Box-Cox plot for power transform, and CD refers to Cook's distance), (d) schematic of RBFNN formulated from the Gaussian function. Reproduced from ref. 149, with permission of ACS OMEGA, copyright 2021.

oxidation state, and metal–support interactions. Co-doping strategies, such as incorporating Ru, improve metal dispersion and enhance the stability of active sites under reaction conditions. The optimization of metal–support interactions, particularly by tuning the metal's d-band structure, is essential for achieving superior catalytic activity and selectivity.

6 Advanced strategies for single-atom catalysts innovation in CO_2 reduction

Recent advancements in SACs have demonstrated their significant potential in enhancing CO_2RR, offering exceptional atomic efficiency and tunable catalytic sites. By maximizing atomic utilization, SACs ensure that each active site corresponds to a single metal atom, thereby substantially enhancing catalytic efficiency compared to conventional nanoparticle-based catalysts. This atomic-level precision, combined with the ability to finely tune the electronic structure and coordination environment of active sites, facilitates efficient CO_2 activation and reduction. SACs have been shown to catalyze the formation of key small organic molecules, such as formate, carbon monoxide, and methane, through mechanisms involving CO_2 adsorption, electron transfer, and bond cleavage.

Despite these promising advancements, a comprehensive mechanistic understanding of SAC-mediated CO_2RR remains incomplete. Current knowledge of precise reaction pathways, the identification of key intermediates, and the role of atomic coordination in determining catalytic activity remains limited. Gaining deeper insights into these mechanistic aspects is crucial for optimizing SACs for large-scale applications. A fundamental understanding of the reaction mechanisms will enable the rational design of SACs with enhanced stability, selectivity, and efficiency-critical attributes for achieving sustainable CO_2RR and contributing to global carbon neutrality objectives.

Furthermore, SACs represent a paradigm shift from conventional catalysts, which typically consist of supported metal or metal oxide nanoparticles. The unique atomic-scale structure of SACs facilitates novel reaction pathways that differ significantly from those of traditional catalysts. These distinct reaction dynamics are crucial for advancing CO_2RR, enabling more efficient conversion and improved product selectivity.

This integrated framework, as shown in Fig. 9, enables the precise design and optimization of SACs, paving the way for scalable and efficient CO_2 conversion.

The performance of SACs is fundamentally governed by their structural design, which directly impacts the catalytic activity and selectivity. This review introduces an innovative approach for CO_2RR, where experimental data guide the selec-

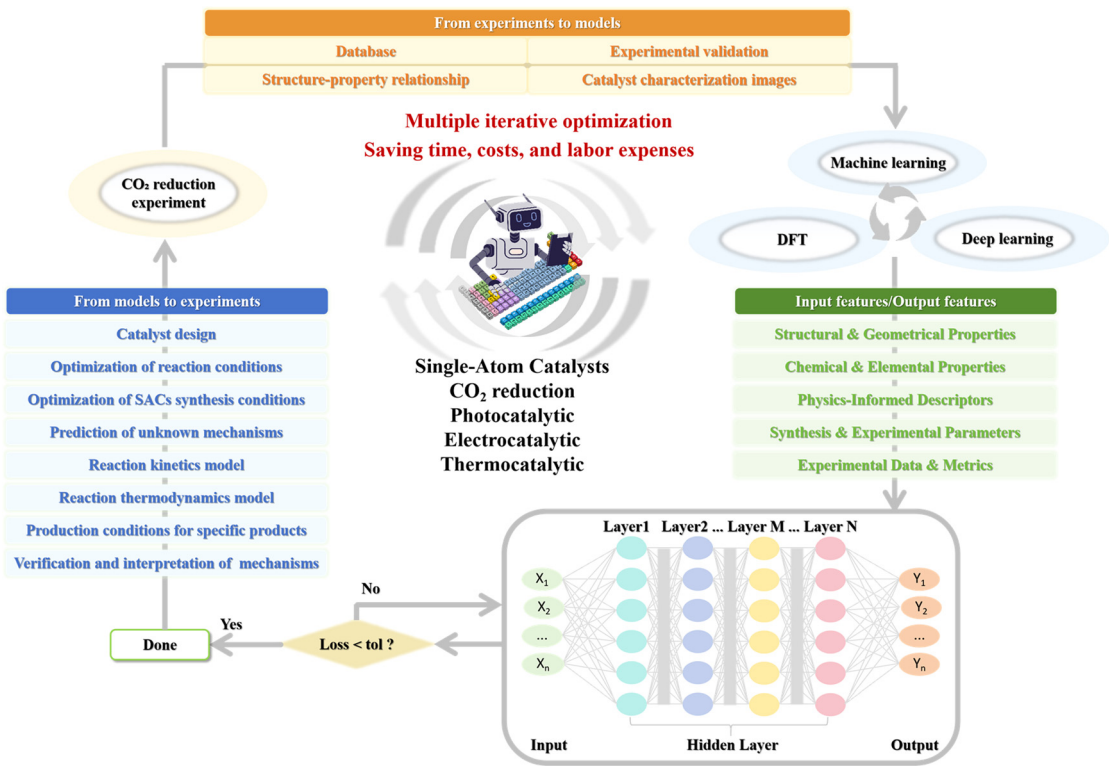

Fig. 9 Holistic iterative optimization framework for CO_2 reduction using single-atom catalysts: integrating advanced machine learning, deep learning, DFT, reaction kinetics and thermodynamic models, high-throughput experimental feedback, and Bayesian optimization for the rational design and enhancement of catalytic performance and mechanistic insights.

tion of reaction conditions, preparation methods of SACs, and key microstructural features. These factors serve as critical parameters in ML models and DFT calculations. By developing mechanistic models based on reaction kinetics and thermodynamics, we aim to iteratively refine active learning models, self-supervised learning frameworks, and large-scale predictive models. In combination with multimodal models, high-throughput experimental data and material characterization results are used to uncover the relationship between the catalyst structure, catalytic properties, reaction pathways, and intermediate selectivity. These efforts reveal previously unexplored CO_2RR mechanisms, providing valuable insights into the rational design of SACs for the highly selective production of target chemicals. Furthermore, by applying Bayesian optimization principles, we propose a strategy to enhance the experimental outcomes, enabling continuous iteration between model predictions and experimental validation.

6.1 Optimization of catalyst synthesis in structure and conditions

The catalytic hydrogenation of CO_2 encompasses multiple pathways, including thermocatalytic, electrocatalytic, photocatalytic, and photo-electrocatalytic reduction. Among these, thermocatalysis has reached a relatively advanced stage of industrial application, while electrocatalytic and photocatalytic systems remain largely confined to laboratory research.

Photocatalysis, inspired by natural photosynthesis, provides an alternative approach for CO_2RR, offering advantages such as low energy consumption and high flexibility. However, photocatalytic systems currently face limitations, including low conversion efficiency and high costs associated with photovoltaic systems. Challenges such as poor interfaces, crystal lattice mismatches, and dangling bonds still limit the performance of photocatalytic and electrocatalytic materials.

Electrocatalysis presents several advantages, including the ability to operate under mild reaction conditions (ambient temperature and pressure) and the flexibility to modulate intermediate species. These features make electrocatalysis a promising option for scalable CO_2RR. However, high costs associated with electrocatalytic systems, particularly expensive materials used in catalysts and electrodes, pose significant barriers to commercialization.

Future research should focus on developing advanced materials to address the fundamental limitations of these systems. For example, low-dimensional semiconducting materials are promising for constructing high-quality interfaces with well-aligned band gaps, facilitating efficient light absorption and charge transfer. The integration of van der Waals heterostructures into photoelectrodes can enhance exciton dissociation, enabling more efficient electron and hole transfer to the catalyst's active sites, thereby improving the overall catalytic performance. Optimizing reaction conditions —such as the temperature, pressure, and CO/H_2 ratio—will be crucial for enhancing the catalytic efficiency of SACs. Particular attention should be paid to the design of new support materials, such as perovskite-based structures, to regulate metal–support interactions. These innovations will enable better control over the electronic properties and coordination environments of SACs, improving the selectivity and efficiency of CO_2 reduction.

Overall, while SACs have shown significant promise in CO_2 hydrogenation and other critical reactions, addressing the remaining challenges related to the cost, reaction conditions, and mechanistic understanding is essential for large-scale implementation of SACs in sustainable CO_2 reduction. Continued improvement in both the fundamental understanding of SACs and the development of new materials will help achieve more efficient, cost-effective, and scalable solutions for CO_2 utilization, advancing scientific innovation and global sustainability goals.

6.2 Machine learning-driven design and pathways of single-atom catalysts for CO_2 reduction

The use of SACs for CO_2 reduction into valuable chemicals has attracted significant attention due to their potential to reduce carbon emissions and store renewable energy. Achieving high selectivity and efficiency in CO_2RR necessitates a comprehensive understanding of the reaction mechanisms, active sites, and intermediate species involved. By integrating ML with DFT calculations, this approach has emerged as a powerful tool for elucidating the reaction mechanisms, optimizing the catalyst design, and predicting reaction pathways.

ML techniques, including DL, active learning, and self-supervised learning, facilitate the prediction of key catalytic properties, such as intermediate adsorption energies, binding affinities, and the electronic structures of SACs. Analyzing large datasets enables ML models to uncover correlations between the catalyst composition, support materials, and catalytic performance, offering valuable insights into designing highly selective SACs for specific high-value CO_2RR products. Notably, ML can guide the design of SACs with tailored properties, such as optimized metal–support interactions and atomic arrangements, thereby improving the reaction pathways and catalytic efficiency.

Integrating ML models with multi-modal data, such as structural and operational information derived from techniques like electron microscopy, further advances the comprehension of catalytic systems. This integration aids in designing SACs with specific properties that optimize the reaction mechanisms and enhance the catalytic performance. For instance, in Cu-based SACs, ML models have been employed to control the morphology of metal nanoparticles, which, in turn, influences the reaction mechanism and product distribution, thereby improving the CO_2RR performance.

Despite the promise of ML in catalyst design, several challenges remain. A major hurdle is the lack of high-quality, annotated datasets for effective ML model training. Data scarcity and experimental noise often lead to inaccurate predictions, hindering the development of optimal catalysts. Furthermore, ML models struggle to capture the full complexity of catalytic systems, especially non-equilibrium effects that influence the SACs stability and reactivity. To overcome these

challenges, future research should focus on expanding and refining datasets through high-throughput experimental techniques and advanced simulations. Hybrid approaches combining data-driven ML methods with first-principles calculations, such as ML-DFT, could further enhance the prediction accuracy and reliability. Another limitation of the current ML models is their limited interpretability. While ML can accurately predict the catalytic properties, understanding the underlying physical mechanisms remains a significant challenge. Enhancing the transparency of ML models through explainable AI techniques is crucial for gaining deeper insights into the catalytic processes and guiding the rational design of SACs with improved performance.

Coupling ML with *operando* techniques, such as X-ray spectroscopy and electron microscopy, facilitates the real-time monitoring of active sites and structural dynamics during reactions. This real-time analysis provides valuable insights into the formation of reaction intermediates and the evolution of active sites throughout the CO_2RR process, offering a deeper understanding of the catalytic behavior of SACs.

While ML models hold great promise for advancing the design and optimization of SACs for CO_2RR, addressing challenges related to the data quality, model interpretability, and system complexity is essential for realizing their full potential. Integrating ML with high-throughput experimentation, advanced simulations, and operando techniques will pave the way for the development of more efficient and selective SACs, ultimately advancing CO_2RR technologies and contributing to global sustainability goals.

6.3 Synergistic optimization of catalysts *via* machine learning and experimental validation

Developing SACs for CO_2RR requires integrating advanced ML, DFT, and experimental validation to enhance the catalyst performance and optimize the reaction pathways. The synergy between predictive models and experimental data provides deeper mechanistic insights, guiding the rational design of SACs with high selectivity and efficiency.

To elucidate the reaction mechanisms of SACs and identify the active phases in CO_2RR, both computational and experimental approaches must be integrated. Computational techniques such as DFT predict the electronic structure of active sites, adsorption energies, and reaction intermediates. By incorporating ML models (*e.g.*, RF, DL, and transformer models), these predictions enable the accurate identification of key catalytic properties and reaction pathways. Optimization of SACs can be achieved by selecting the appropriate descriptors for catalysts, auxiliary agents, and support materials, with a focus on tailoring the spatial structure to enhance the catalytic performance.

Bayesian theory provides a robust framework for constructing thermodynamic and kinetic models based on experimental data, facilitating the prediction of highly selective, efficient, and stable SACs. Integrating these predictions with experimental validation enables iterative model refinement. Incorporating new experimental data enhances the predictive accuracy, facilitating the development of more precise models. This continuous feedback loop between the computational predictions and experimental testing is crucial for uncovering previously unknown reaction pathways and optimizing SACs for CO_2RR. Furthermore, by continuously updating models with new data and refining reaction mechanisms, optimal reaction conditions for specific products can be predicted. The iterative optimization process enables tailored SACs design, adjusting the catalyst structures and reaction environments based on the desired product distribution.

The dynamic interplay between the ML predictions, DFT simulations, and experimental validation accelerates SACs development, ensuring more efficient and selective CO_2RR. The continuous refinement of computational models and experimental methodologies deepens mechanistic understanding, facilitates the design of highly selective SACs, and optimizes reaction conditions, ultimately advancing scalable catalytic applications.

7 Conclusion

SACs have shown great potential in CO_2RR due to atomically dispersed active sites, which allow for tunable catalytic properties. However, further development is necessary to fully understand the reaction mechanisms, optimize conditions, and scale up the catalysts. The integration of DFT, ML, and experimental validation holds immense promise for designing next-generation SACs with improved efficiency, selectivity, and stability.

1. The synergy between DFT and ML has greatly advanced the SACs design for CO_2RR. DFT provides insights into the electronic structure and reaction intermediates, while ML optimizes the catalyst properties, predicts the reaction pathways, and tailors the SACs functionalities to enhance both efficiency and selectivity.

2. Iterative ML refinement through continuous experimental validation creates a dynamic feedback loop, progressively improving SACs. Integrating experimental data enhances the prediction accuracy, enabling the design of SACs with superior stability and selectivity for specific products.

3. Achieving deeper mechanistic understanding requires precise identification of active sites. Combining ML, DFT, and experimental techniques helps elucidate complex reaction pathways, optimizing the SACs coordination environments and improving selectivity.

4. The SACs design must account for the different reaction conditions, such as temperature, pressure, and CO/H_2 ratios. Fine-tuning these parameters alongside well-designed SACs enhances the catalytic performance and stability under practical conditions.

5. Multimodal modeling, combining DFT structural descriptors with experimental data, allows for precise control over the SACs active sites and configurations, facilitating the development of highly active and scalable catalysts for industrial CO_2RR applications.

These advancements are crucial for realizing practical CO_2RR technologies and achieving global sustainability goals.

Data availability

No primary research results, software or code have been included, and no new data were generated or analysed as part of this review.

Conflicts of interest

There are no conflicts to declare.

Acknowledgements

We ackowledge the financial support from China NSFC No.22276026 received by Prof. Lifen Liu.

References

1 T. J. Wang, W. S. Fang, Y. M. Liu, F. M. Li, P. Chen and Y. Chen, Heterostructured Pd/PdO nanowires for selective and efficient CO_2 electroreduction to CO, *Energy Chem.*, 2022, **70**, 407–413.
2 W. Wang, Z. Ma, X. Fei, X. Wang, Z. Yang, Y. Wang, J. Q. Zhang, H. Ning, N. Tsubaki and M. B. Wu, Joint tuning the morphology and oxygen vacancy of Cu_2O by ionic liquid enables high-efficient CO_2 reduction to C_2 products, *Chem. Eng. J.*, 2022, **436**, 135029.
3 W. Wang, X. Wang, Z. Ma, Y. Wang, Z. Yang, J. Zhu, L. Lv, H. Ning, N. Tsubaki and M. Wu, Carburized In_2O_3 Nanorods Endow CO_2 Electroreduction to Formate at 1 A cm^{-2}, *ACS Catal.*, 2022, **13**, 796–802.
4 Y. Yang, S. Louisia, S. Yu, J. Jin, I. Roh, C. Chen, M. V. Fonseca Guzman, J. Feijóo, *et al.*, Operando studies reveal active Cu nanograins for CO_2 electroreduction, *Nature*, 2023, **614**, 262–269.
5 Z. Feng, X. Zhu, J. Yang, K. Zhong, Z. Jiang, Q. Yu, Y. Song, Y. Hua, H. Li and H. Xu, Inherent Facet-Dominant effect for cobalt oxide nanosheets to enhance photocatalytic CO_2 reduction, *Appl. Surf. Sci.*, 2022, **578**, 151848.
6 R. Murakami, K. Shiota, A. Uchida and F. Inagaki, Light-swing CO_2 capture: photoirradiation-based chemical CO_2 release based on photoisomerization of azobenzene-amine/guanidine derivatives, *Green Chem.*, 2024, **26**, 7406.
7 S. S. Satter, J. S. Lopez, M. L. Hubbard, Y. Jiang, R. A. Dagle and J. Kothandaraman, Reactive direct air capture of CO_2 to C-C coupled products using multifunctional materials, *Green Chem.*, 2024, **26**, 8242–8255.
8 J. X. Gu, X. Zhao, Y. Sun, J. Zhou, C. Y. Sun, X. L. Wang, Z. H. Kang and Z. M. Su, A photo-activated process cascaded electrocatalysis for the highly efficient CO_2 reduction over a core–shell ZIF-8@Co/C, *J. Mater. Chem. A*, 2020, **8**, 16616–16623.
9 L. Ye, Y. Ying, D. Sun, Z. Zhang, L. Fei, Z. Wen, J. Qiao and H. Huang, Highly Efficient Porous Carbon Electrocatalyst with Controllable N–Species Content for Selective CO_2 Reduction, *Angew. Chem., Int. Ed.*, 2020, **59**, 3244–3251.
10 C. X. Zhao, J. N. Liu, B. Q. Li, D. Ren, X. Chen, J. Yu and Q. Zhang, Multiscale Construction of Bifunctional Electrocatalysts for Long-Lifespan Rechargeable Zinc-Air Batteries, *Adv. Funct. Mater.*, 2020, **36**, 2003619.
11 Y. Zhou, Z. Wang, L. Huang, S. Zaman, K. Lei, T. Yue, Z. Li, B. You and B. Y. Xia, Engineering 2D Photocatalysts toward Carbon Dioxide Reduction, *Adv. Energy Mater.*, 2021, **11**, 2003159.
12 O. S. Bushuyev, P. D. Luna, C. T. Dinh, J. Lagemaat, S. O. Kelley and E. H. Sargent, What Should We Make with CO_2 and How Can We Make It?, *Joule*, 2018, **2**, 825–832.
13 J. M. Spurgeon and B. A. Kumar, comparative technoeconomic analysis of pathways for commercial electrochemical CO_2 reduction to liquid products, *Energy Environ. Sci.*, 2018, **11**, 1536–1551.
14 Y. Y. Birdja, E. Pérez-Gallent, M. C. Figueiredo, A. J. Göttle, F. Calle-Vallejo and M. T. M. Koper, Advances and challenges in understanding the electrocatalytic conversion of carbon dioxide to fuels, *Nat. Energy*, 2019, **4**, 732–745.
15 C. Wang, Z. Sun, Y. Zheng and Y. H. Hu, Recent progress in visible light photocatalytic conversion of carbon dioxide, *J. Mater. Chem. A*, 2019, **7**, 865–887.
16 C. Jiang, S. J. A. Moniz, A. Wang, T. Zhang and J. Tang, Photoelectrochemical devices for solar water splitting-materials and challenges, *Chem. Soc. Rev.*, 2017, **46**, 4645–4660.
17 D. Voiry, H. S. Shin, K. P. Loh and M. Chhowalla, Low-dimensional catalysts for hydrogen evolution and CO_2 reduction, *Nat. Rev. Chem.*, 2018, **2**, 0105.
18 B. Qiao, A. Wang, X. Yang, L. F. Allard, Z. Jiang, Y. Cui, J. Liu, J. Li and T. Zhang, Single-atom catalysis of CO oxidation using Pt_1/FeO_x, *Nat. Chem.*, 2011, **3**, 634–641.
19 Y. Xiong, W. Sun, Y. Han, P. Xin, X. Zheng, W. Yan, J. Dong, J. Zhang, D. Wang and Y. Li, Cobalt single atom site catalysts with ultrahigh metal loading for enhanced aerobic oxidation of ethylbenzene, *Nano Res.*, 2021, **14**, 2418–2423.
20 Y. Xiong, W. Sun, P. Xin, W. Chen, X. Zheng, W. Yan, L. Zheng, J. Dong, J. Zhang, D. Wang and Y. Li, Gram-Scale Synthesis of High-Loading Single-Atomic-Site Fe Catalysts for Effective Epoxidation of Styrene, *Adv. Mater.*, 2020, **32**, 2000896.
21 B. H. Lee, S. Park, M. Kim, *et al.*, Reversible and cooperative photoactivation of single-atom Cu/TiO_2 photocatalysts, *Nat. Mater.*, 2019, **18**, 620–626.
22 J. H. Wang, M. S. Yin, Q. Zhang, F. Cao, Y. Xing, Q. Zhao, Y. Wang, W. Xu, W. Wu and M. Wu, Single-Atom Fe-N_4 sites promote the triplet-energy transfer process of g-C_3N_4 for the photooxidation, *J. Catal.*, 2021, **404**, 89–95.
23 H. Ou, D. Wang and Y. Li, How to select effective electrocatalysts: Nano or single atom?, *Nano Select*, 2021, **2**, 492–511.

24 Q. N. Zhan, T. Y. Shuai, H. M. Xu, C. J. Huang, Z. J. Zhang and G. R. Li, Syntheses and applications of single-atom catalysts for electrochemical energy conversion reactions, *Chin. J. Catal.*, 2023, **47**, 32–66.
25 Q. Sun, C. Jia, Y. Zhao and C. Zhao, Single atom-based catalysts for electrochemical CO_2 reduction, *Chin. J. Catal.*, 2022, **43**, 1547–1597.
26 L. Wang, S. Lyu and S. Li, *In situ* observation of structural evolution of single-atom catalysts: From synthesis to catalysis, *ChemPhysMater*, 2024, **3**, 24–35.
27 M. Zhong, K. Tran, Y. Min, C. Wang, Z. Wang, C. T. Dinh, P. D. Luna, Z. Yu, A. S. Rasouli, P. Brodersen, S. Sun, O. Voznyy, C. S. Tan, M. Askerka, F. Che, M. Liu, A. Seifitokaldani, Y. Pang, S.-C. Lo, A. Ip, Z. Ulissi and E. H. Sargent, Accelerated discovery of CO_2 electrocatalysts using active machine learning, *Nature*, 2020, **581**, 178–183.
28 Y. Yang, S. Louisia, S. Yu, J. Jin, I. Roh, C. Chen, M. V. Fonseca Guzman, J. Feijóo, P. C. Chen, H. Wang, C. J. Pollock, X. Huang, Y. T. Shao, C. Wang, D. A. Muller, H. D. Abruña and P. Yang, Operando studies reveal active Cu nanograins for CO_2 electroreduction, *Nature*, 2023, **614**, 262–269.
29 W. Fang, W. Guo, R. Lu, Y. Yan, X. Liu, D. Wu, F. M. Li, Y. Zhou, C. He, C. Xia, H. Niu, S. Wang, Y. Liu, Y. Mao, C. Zhang, B. You, Y. Pang, L. Duan, X. Yang, F. Song, T. Zhai, G. Wang, X. Guo, B. Tan, T. Yao, Z. Wang and B. Y. Xia, Durable CO_2 conversion in the proton-exchange membrane system, *Nature*, 2024, **626**, 86–91.
30 Y. Xiao, H. T. Zhang and M. T. Zhang, Heterobimetallic NiFe Complex for Photocatalytic CO_2 Reduction: United Efforts of NiFe Dual Sites, *J. Am. Chem. Soc.*, 2024, **146**, 28832–28844.
31 Z. Wu, J. Liu, B. Mu, X. Xu, W. Sheng, W. Tao and Z. Li, Machine-Learning assisted screening of double metal catalysts for CO_2 electroreduction to CH_4, *Appl. Surf. Sci.*, 2024, **648**, 159027.
32 Y. Li, S. Wang, Z. Lv, Z. Wang, Y. Zhao, Y. Xie, Y. Xu, L. Qian, Y. Yang, Z. Zhao and J. Zhang, Transforming the synthesis of carbon nanotubes with machine learning models and automation, *Matter*, 2025, **8**, 101913.
33 V. Sumaria, T. B. Rawal, Y. F. Li, D. Sommer, J. Vikoren, R. J. Bondi, M. Rupp, A. Prasad and D. Prasad, Machine Learning, Density Functional Theory, and Experiments to Understand the Photocatalytic Reduction of CO_2 on CuPt/TiO_2, *J. Phys. Chem. C*, 2024, **128**, 14247–14258.
34 J. Liu, Y. Cai, R. Song, S. Ding, Z. Lyu, Y.-C. Chang, H. Tian, X. Zhang, D. Du, W. Zhu, Y. Zhou and Y. Lin, Recent progress on single-atom catalysts for CO_2 electroreduction, *Mater. Today*, 2021, **48**, 95–114.
35 X. F. Ziang Shang, G. Chen, R. Qin and Y. Han, Recent Advances on Single-Atom Catalysts for Photocatalytic CO_2 Reduction, *Small*, 2023, **19**, 2304975.
36 W. Hu, H. Yang and C. Wang, Progress in photocatalytic CO_2 reduction based on single-atom catalysts, *RSC Adv.*, 2023, **13**, 20889–20908.
37 J. Lin, B. Qiao, J. Liu, Y. Huang, A. Wang, L. Li, W. Zhang, L. F. Allard, X. Wang and T. Zhang, Design of a Highly Active Ir/Fe$(OH)_x$ Catalyst: Versatile Application of Pt-Group Metals for the Preferential Oxidation of Carbon Monoxide, *Angew. Chem., Int. Ed.*, 2012, **51**, 2920–2924.
38 B. J. O'Neill, D. H. K. Jackson, J. Lee, C. Canlas, P. C. Stair, C. L. Marshall, J. W. Elam, T. F. Kuech, J. A. Dumesic and G. W. Huber, Catalyst Design with Atomic Layer Deposition, *ACS Catal.*, 2015, **5**, 1804–1825.
39 S. Sun, G. Zhang, N. Gauquelin, N. Chen, J. Zhou, S. Yang, W. Chen, X. Meng, D. Geng, *et al.*, Single-atom catalysis using Pt/graphene achieved through atomic layer deposition, *Sci. Rep.*, 2013, **3**, 1775.
40 L. Zhang, Z. J. Zhao and J. Gong, Nanostructured Materials for Heterogeneous Electrocatalytic CO_2 Reduction and their Related Reaction Mechanisms, *Angew. Chem., Int. Ed.*, 2017, **56**, 11326.
41 T. Ouyang, H. H. Huang, J. W. Wang, D. C. Zhong and T. B. Lu, A Dinuclear Cobalt Cryptate as a Homogeneous Photocatalyst for Highly Selective and Efficient Visible-Light Driven CO_2 Reduction to CO in CH_3CN/H_2O Solution, *Angew. Chem.*, 2017, **129**, 756–761.
42 C. Zhu, S. Fu, Q. Shi, D. Du and Y. Lin, Single-atom electrocatalysts, *Angew. Chem., Int. Ed.*, 2017, **56**, 13944.
43 Y. Wang, P. Han, X. Lv, L. Zhang and G. Zheng, Defect and Interface Engineering for Aqueous Electrocatalytic CO_2 Reduction, *Joule*, 2018, **12**, 2551–2582.
44 N. Corbin, J. Zeng, K. Williams and K. Manthiram, Heterogeneous molecular catalysts for electrocatalytic CO_2 reduction, *Nano Res.*, 2019, **12**, 2093–2125.
45 Z. Yang, W. Gao and Q. Jiang, A machine learning scheme for the catalytic activity of alloys with intrinsic descriptors, *J. Mater. Chem. A*, 2020, **8**, 17507–17515.
46 K. Tran and Z. W. Ulissi, Active learning across intermetallics to guide discovery of electrocatalysts for CO_2 reduction and H_2 evolution, *Nat. Catal.*, 2018, **1**, 696–703.
47 M. Zhong, K. Tran, Y. Min, C. Wang, Z. Wang, C. T. Dinh, P. De Luna, Z. Yu, A. S. Rasouli, P. Brodersen, S. Sun, O. Voznyy, C. S. Tan, M. Askerka, F. Che, M. Liu, A. Seifitokaldani, Y. Pang, S. C. Lo, A. Ip, Z. Ulissi and E. H. Sargent, Accelerated discovery of CO_2 electrocatalysts using active machine learning, *Nature*, 2020, **581**, 178–183.
48 W. Gao, Y. Chen, B. Li, S. P. Liu, X. Liu and Q. Jiang, Determining the adsorption energies of small molecules with the intrinsic properties of adsorbates and substrates, *Nat. Commun.*, 2020, **11**, 1196.
49 X. Ma, Z. Li, L. E. Achenie and H. Xin, Machine-Learning-Augmented Chemisorption Model for CO_2 Electroreduction Catalyst Screening, *J. Phys. Chem. Lett.*, 2015, **6**, 3528–3533.
50 X. Wan, Z. Zhang, H. Niu, Y. Yin, C. Kuai, J. Wang, C. Shao and Y. Guo, Machine-Learning-Accelerated Catalytic Activity Predictions of Transition Metal Phthalocyanine Dual-Metal-Site Catalysts for CO_2 Reduction, *J. Phys. Chem. Lett.*, 2021, **12**, 6111–6118.

51 S. Özsoysal, B. Oral and R. Yıldırım, Analysis of photocatalytic CO_2 reduction over MOFs using machine learning, *J. Mater. Chem. A*, 2024, **12**, 5748–5759.
52 Q. Yang, L. Zhao, R. Bao, Y. Fan, J. Zhou, D. Rong, H. Zhou and D. Zhang, Interpretable machine learning-assisted advanced exergy optimization for carbon-neutral olefins production, *Renewable Sustainable Energy Rev.*, 2025, **208**, 115027.
53 H. Sun and J. Y. Liu, Advancing CO_2RR with O-Coordinated Single-Atom Nanozymes: A DFT and Machine Learning Exploration, *ACS Catal.*, 2024, **14**, 14021–14030.
54 L.-H. Mou, J. Du, Y. Li, J. Jiang and L. Chen, Effective Screening Descriptors of Metal-Organic Framework-Supported Single-Atom Catalysts for Electrochemical CO_2 Reduction Reactions: A Computational Study, *ACS Catal.*, 2024, **14**, 12947–12955.
55 R. Ding, J. Chen, Y. Chen, J. Liu, Y. Bando and X. Wang, Unlocking the potential: machine learning applications in electrocatalyst design for electrochemical hydrogen energy transformation, *Chem. Soc. Rev.*, 2024, **53**, 11390–11461.
56 M. Sun and B. Huang, Direct Machine Learning Predictions of C_3 Pathways, *Adv. Energy Mater.*, 2024, **14**, 2400152.
57 J. Ock, S. Badrinarayanan, R. Magar, A. Antony and A. B. Farimani, Multimodal language and graph learning of adsorption configuration in catalysis, *Nat. Mach. Intell.*, 2024, **6**, 1501–1511.
58 M. Ren, X. Guo, S. Zhang and S. Huang, Design of Graphdiyne and Holey Graphyne-Based Single Atom Catalysts for CO_2 Reduction With Interpretable Machine Learning, *Adv. Funct. Mater.*, 2023, **33**, 2213543.
59 X. Bai, Y. Li, Y. Xie, Q. Chen, X. Zhang and J. R. Li, High-throughput screening of CO_2 cycloaddition MOF catalyst with an explainable machine learning model, *Green Energy Environ.*, 2025, **10**, 132–138.
60 L. Wang, H. Chen, L. Yang, J. Li, Y. Li and X. Wang, Single-atom catalysts property prediction via Supervised and Self-Supervised pre-training models, *Chem. Eng. J.*, 2024, **487**, 150626.
61 Q. Zhu, Y. Gu, X. Liang, X. Wang and J. Ma, A Machine Learning Model to Predict CO_2 Reduction Reactivity and Products Transferred from Metal-Zeolites, *ACS Catal.*, 2022, **12**, 12336–12348.
62 A. S. Varela, N. Ranjbar Sahraie, J. Steinberg, W. Ju, H. S. Oh and P. Strasser, Metal-Doped Nitrogenated Carbon as an Efficient Catalyst for Direct CO_2 Electroreduction to CO and Hydrocarbons, *Angew. Chem.*, 2015, **127**, 10908–10912.
63 R. Guo, C. Guo, Z. Bi, H. Zhang, N. Lv, B. Xi, G. Hu and J. Xu, The single atom Fe loaded catalytic membrane for effective peroxymonosulfate activation and pollution degradation, *Appl. Catal., B*, 2024, **356**, 124243.
64 A. V. Bukhtiyarov, M. A. Panafidin, I. P. Prosvirin, N. S. Smirnova, P. V. Markov, G. N. Baeva, I. S. Mashkovsky, G. O. Bragina, C. Rameshan, E. Yu. Gerasimov, Y. V. Zubavichus, V. I. Bukhtiyarov and A. Yu. Stakheev, Deliberate control of the structure-specific active sites in PdIn bimetallic catalysts using adsorbate induced segregation effects, *Appl. Surf. Sci.*, 2023, **608**, 155–086.
65 G. A. Naikoo, F. Arshad, I. U. Hassan, F. B. Omar, M. M. Tambuwala, M. Mustaqeem and T. A. Saleh, Trends in bimetallic nanomaterials and methods for fourth-generation glucose sensors, *Trends Anal. Chem.*, 2023, **162**, 117042.
66 S. K. Lahiri, C. Zhang, M. Sillanpää and L. Liu, NiO@SiO_2 photo-catalyst prepared by ion-exchange method for fast elimination of reactive dyes from wastewater, *Mater. Today Chem.*, 2022, **23**, 100–677.
67 A. Kowalczyk, A. Borcuch, M. Michalik, M. Rutkowska, B. Gil, Z. Sojka, P. Indyka and L. Chmielarz, MCM-41 modified with transition metals by template ion-exchange method as catalysts for selective catalytic oxidation of ammonia to dinitrogen, *Microporous Mesoporous Mater.*, 2017, **240**, 9–21.
68 V. Andrei, I. Roh, J. A. Lin, J. Lee, Y. Shan, C. K. Lin, S. Shelton, E. Reisner and P. Yang, Perovskite-driven solar C_2 hydrocarbon synthesis from CO_2, *Nat. Catal.*, 2025, 137–146.
69 K. Maeda, D. An, R. Kuriki, D. Lu and O. Ishitani, Graphitic carbon nitride prepared from urea as a photocatalyst for visible-light carbon dioxide reduction with the aid of a mononuclear ruthenium(II) complex, *J. Org. Chem.*, 2018, **14**, 1806–1812.
70 W. Zhang, Z. Jin and Z. Chen, Rational-Designed Principles for Electrochemical and Photoelectrochemical Upgrading of CO_2 to Value-Added Chemicals, *Adv. Sci.*, 2022, **9**, 2105204.
71 X. Tao, Y. Wang, J. Qu, Y. Zhao, R. Li and C. Li, Achieving selective photocatalytic CO_2 reduction to CO on bismuth tantalum oxyhalogen nanoplates, *J. Mater. Chem. A*, 2021, **9**, 19631–19636.
72 X. M. You, B. Xu, H. Zhou, H. Qiao, X. Lv, Z. Huang, J. Pang, L. Yang, P. F. Liu, X. Guan, H. G. Yang, X. Wang and Y. F. Yao, Ultrahigh Bifunctional Photocatalytic CO_2 Reduction and H_2 Evolution by Synergistic Interaction of Heteroatomic Pt-Ru Dimerization Sites, *ACS Nano*, 2024, **18**, 9403–9412.
73 A. Fujishima and K. Honda, Electrochemical photolysis of water at a semiconductor electrode, *Nature*, 1972, **238**, 37–38.
74 M. Halmann, Photoelectrochemical reduction of aqueous carbon dioxide on p-type gallium phosphide in liquid junction solar cells, *Nature*, 1978, **275**, 115–116.
75 J. Xia, N. Karjule, B. Mondal, J. Qin, M. Volokh, L. Xing and M. Shalom, Design of melem-based supramolecular assemblies for the synthesis of polymeric carbon nitrides with enhanced photocatalytic activity, *J. Mater. Chem. A*, 2021, **9**, 17855–17864.
76 J. Wu, Y. Huang, W. Ye and Y. Li, CO_2 Reduction: From the Electrochemical to Photochemical Approach, *Adv. Sci.*, 2017, **4**, 1700194.
77 H. Zhang, Y. Wang, S. Zuo, W. Zhou, J. Zhang and X. W. D. Lou, Isolated Cobalt Centers on $W_{18}O_{49}$

Nanowires Perform as a Reaction Switch for Efficient CO_2 Photoreduction, *Chem. Soc.*, 2021, **143**, 2173–2177.
78 Y. Li, S. Wang, X. Wang, Y. He, Q. Wang, Y. Li, M. Li, G. Yang, J. Yi, H. Lin, D. Huang, L. Li, H. Chen and J. Ye, Facile top-down strategy for direct metal atomization and coordination achieving a high turnover number in CO_2 Photoreduction, *J. Am. Chem. Soc.*, 2020, **142**, 19259–19267.
79 C. Feng, T. T. Bo, P. Maity, S. W. Zuo, W. Zhou, K. W. Kuang, O. F. Mohammed and H. Zhang, Regulating Photocatalytic CO_2 Reduction Kinetics through Modification of Surface Coordination Sphere, *Adv. Funct. Mater.*, 2024, **34**, 2309761.
80 Y. Zhang, B. Johannessen, P. Zhang, J. Gong, J. Ran and S. Z. Qiao, Reversed Electron Transfer in Dual Single Atom Catalyst for Boosted Photoreduction of CO_2, *Adv. Mater.*, 2023, **35**, 2306923.
81 H. Haroon and Q. Xiang, Single-Atom based Metal-Organic Framework Photocatalysts for Solar-Fuel Generation, *Small*, 2024, **20**, 2401389.
82 Y. Wang, L. Liao, G. Zhu, W. Xie, Q. Zhou, F. Yu, H. Zhou and H. Zhou, Metal-nitrogen coordinated single atomic photocatalysts for solar energy conversion, *Coord. Chem. Rev.*, 2025, **523**, 216254.
83 Q. Yang, H. Liu, Y. Lin, D. Su, Y. Tang and L. Chen, Atomically Dispersed Metal Catalysts for the Conversion of CO_2 into High-Value C_{2+} Chemicals, *Adv. Mater.*, 2024, **36**, 2310912.
84 Y. Zheng, W. Li, J. Ju, J. Jiang, L. Zhang, H. Jiang, Y. Hu and C. Li, Oxygen vacancy mediated Pd-SA/TiO_2 single-atom catalyst created via ultra-fast one-step synthesis for enhanced CO_2 photoreduction, *J. Colloid Interface Sci.*, 2025, **683**, 280–290.
85 B. Rhimi, M. Zhou, Z. Yan, X. Cai and Z. Jiang, Cu-Based Materials for Enhanced C_{2+} Product Selectivity in Photo-/Electro-Catalytic CO_2 Reduction: Challenges and Prospects, *Nano-Micro Lett.*, 2024, **16**, 64.
86 Y. Luo, X. Wang, F. Gao, L. Jiang, D. Wang and H. Pan, From Single Atom Photocatalysts to Synergistic Photocatalysts: Design Principles and Applications, *Adv. Funct. Mater.*, 2024, 2418427.
87 W. Lyu, Y. Liu, J. Zhou, D. Chen, X. Zhao, R. Fang, F. Wang and Y. Li, Modulating the Reaction Configuration by Breaking the Structural Symmetry of Active Sites for Efficient Photocatalytic Reduction of Low-concentration CO_2, *Angew. Chem., Int. Ed.*, 2023, **62**, e202310733.
88 Z. W. Huang, K. Q. Hu, X. B. Li, Z. N. Bin, Q. Y. Wu, Z. H. Zhang, Z. J. Guo, W. S. Wu, Z. F. Chai, L. Mei and W. Q. Shi, Thermally Induced Orderly Alignment of Porphyrin Photoactive Motifs in Metal–Organic Frameworks for Boosting Photocatalytic CO_2 Reduction, *J. Am. Chem. Soc.*, 2023, **145**, 18148–18159.
89 L. Cheng, H. Yin, C. Cai, J. Fan and Q. Xiang, Single Ni Atoms Anchored on Porous Few–Layer g–C_3N_4 for Photocatalytic CO_2 Reduction: The Role of Edge Confinement, *Small*, 2020, **16**, 2002411.
90 P. Zhang, X. Zhan, L. Xu, X. Fu, T. Zheng, X. Yang, Q. Xu, D. Wang, D. Qi, T. Sun and J. Jiang, Mass production of a single-atom cobalt photocatalyst for high-performance visible-light photocatalytic CO_2 reduction, *J. Mater. Chem. A*, 2021, **9**, 26286–26297.
91 A. Wang, J. Li and T. Zhang, Heterogeneous single-atom catalysis, *Nat. Rev. Chem.*, 2018, **2**, 65–81.
92 P. Zhang, X. Zhan, L. Xu, X. Fu, T. Zheng, X. Yang, Q. Xu, D. Wang, D. Qi, T. Sun and J. Jiang, Mass production of a single-atom cobalt photocatalyst for high-performance visible-light photocatalytic CO_2 reduction, *J. Mater. Chem. A*, 2021, **9**, 26286–26297.
93 J. Lee, G. I. N. Waterhouse, Y. Mao, Z. Wang, E. Zhu, J. Low, S. P. Chai and L. L. Tan, Lead-free halide perovskites and Bi-BTC frameworks: Engineering S-scheme heterojunctions for photocatalytic CO_2 conversion, *Appl. Catal., B*, 2025, **365**, 124942.
94 J. He, X. Wang, P. Feng, Y. Zhou, K. Wang, B. Zou and M. Zhu, Isostructural phase transition-induced piezoelectricity in all-inorganic perovskite $CsPbBr_3$ for catalytic CO_2 reduction, *Appl. Catal., B*, 2024, **355**, 124186.
95 Y. Feng, D. Chen, M. Niu, Y. Zhong, Z. He, S. Ma, K. Yuan, H. Ding, K. Lv, L. Guo, W. Zhang and M. Ma, Ligand free synthesis of atomically dispersed Cu doping ultrathin $Cs_3Bi_2Br_9$ for efficient photoreduction CO_2 with high CO selectivity, *Appl. Catal., B*, 2025, **365**, 124931.
96 Z. L. Liu, Y. F. Mu, X. R. Li, Y. X. Feng, M. Zhang and T. B. Lu, Constructing strong built-in electric field in lead-free halide-perovskite-based heterojunction to boost charge separation for efficient CO_2 photoreduction, *Appl. Catal., B*, 2025, **366**, 125012.
97 H. Sun, Z. Lin, R. Tang, Y. Liang, S. Zou, X. Zhang, K. Chen, R. Zheng and J. Huang, Enhanced solar urea synthesis from CO_2 and nitrate waste via oxygen vacancy mediated-TiO_x support lead-free perovskite, *Appl. Catal., B*, 2025, **360**, 124511.
98 Q. Lu, J. Rosen, Y. Zhou, G. S. Hutchings, Y. C. Kimmel, J. G. Chen and F. Jiao, A selective and efficient electrocatalyst for carbon dioxide reduction, *Nat. Commun.*, 2014, **5**, 32–42.
99 B. Zhang and J. Zhang, Rational design of Cu-based electrocatalysts for electrochemical reduction of carbon dioxide, *Energy Chem.*, 2017, **26**, 1050–1066.
100 J. He, N. J. J. Johnson, A. Huang and C. P. Berlinguette, Electrocatalytic Alloys for CO_2 Reduction, *ChemSusChem*, 2018, **11**, 48–57.
101 Q. Hao, Q. Tang, H. X. Zhong, J. Z. Wang, D. X. Liu and X. B. Zhang, Fully exposed nickel clusters with electron-rich centers for high-performance electrocatalytic CO_2 reduction to CO, *Sci. Bull.*, 2022, **67**, 1477–1485.
102 S. Liu, H. B. Yang, S. F. Hung, J. Ding, W. Cai, L. Liu, J. Gao, X. Li, X. Ren, Z. Kuang, Y. Huang, T. Zhang and B. Liu, Elucidating the Electrocatalytic CO_2 Reduction Reaction over a Model Single–Atom Nickel Catalyst, *Angew. Chem., Int. Ed.*, 2019, **59**, 798–803.

103 H. Gu, J. Wu and L. Zhang, Recent advances in the rational design of single-atom catalysts for electrochemical CO_2 reduction, *Nano Res.*, 2022, **15**, 9747–9763.
104 N. Qiu, J. Li, H. Wang and Z. Zhang, Emerging dual-atomic-site catalysts for electrocatalytic CO_2 reduction, *Sci. China Mater.*, 2022, **65**, 3302–3323.
105 Y. Li, Z. He, F. Wu, S. Wang, Y. Cheng and S. Jiang, Defect engineering of high-loading single-atom catalysts for electrochemical carbon dioxide reduction, *Mater. Rep. Energy*, 2023, **3**, 100197.
106 D. Gao, T. Liu, G. Wang and X. Bao, Structure Sensitivity in Single-Atom Catalysis toward CO_2 Electroreduction, *ACS Energy Lett.*, 2021, **6**, 713–727.
107 Y. E. Kim, Y. N. Ko, B. S. An, J. Hong, Y. E. Jeon, H. J. Kim, S. Lee, J. Lee and W. Lee, Atomically Dispersed Nickel Coordinated with Nitrogen on Carbon Nanotubes to Boost Electrochemical CO_2 Reduction, *Energy Lett.*, 2023, **8**, 3288–3296.
108 Y. Wang, Y. Liu, W. Liu, J. Wu, Q. Li, Q. Feng, Z. Chen, X. Xiong, D. Wang and Y. Lei, Regulating the coordination structure of metal single atoms for efficient electrocatalytic CO_2 reduction, *Energy Environ. Sci.*, 2020, **13**, 4609–4624.
109 S. Yang, H. An, S. Arnouts, H. Wang, X. Yu, J. de. Ruiter, S. Bals, T. Altantzis, B. M. Weckhuysen and W. V. D. Stam, Halide-guided active site exposure in bismuth electrocatalysts for selective CO_2 conversion into formic acid, *Nat. Catal.*, 2023, **6**, 796–806.
110 J. Feng, L. Zhang, S. Liu, L. Xu, X. Ma, X. Tan, L. Wu, Q. Qian, T. Wu, J. Zhang, X. Sun and B. Han, Modulating adsorbed hydrogen drives electrochemical CO_2-to-C_2 products, *Nat. Commun.*, 2023, **14**, 4615.
111 Z. Jin, M. Yang, Y. Dong, X. Ma, Y. Wang, J. Wu, J. Fan, D. Wang, R. Xi, X. Zhao, T. Xu, J. Zhao, *et al.*, Atomic Dispersed Hetero-Pairs for Enhanced Electrocatalytic CO_2 Reduction, *Nano-Micro Lett.*, 2024, **16**, 4.
112 Y. Cao, S. Chen, S. Bo, W. Fan, J. Li, C. Jia, Z. Zhou, Q. Liu, L. Zheng and F. Zhang, Single Atom Bi Decorated Copper Alloy Enables C-C Coupling for Electrocatalytic Reduction of CO_2 into C_{2+} Products, *Angew. Chem.*, 2023, **135**, e202303048.
113 F. Cai, D. Gao, H. Zhou, G. Wang, T. He, H. Gong, S. Miao, F. Yang, J. Wang and X. Bao, Electrochemical promotion of catalysis over Pd nanoparticles for CO_2 reduction, *Chem. Sci.*, 2017, **8**, 2569–2573.
114 Y. Quan, R. Yu, J. Zhu, A. Guan, X. Lv, C. Yang, S. Li, J. Wu and G. Zheng, Efficient carboxylation of styrene and carbon dioxide by single-atomic copper electrocatalyst, *J. Colloid Interface Sci.*, 2021, **601**, 378–384.
115 J. Rosen, G. S. Hutchings, Q. Lu, R. V. Forest, A. Moore and J. Feng, Electrodeposited Zn Dendrites with Enhanced CO Selectivity for Electrocatalytic CO_2 Reduction, *ACS Catal.*, 2015, **5**, 4586–4591.
116 Y. Chen and M. W. Kanan, Tin Oxide Dependence of the CO_2 Reduction Efficiency on Tin Electrodes and Enhanced Activity for Tin/Tin Oxide Thin-Film Catalysts, *J. Am. Chem. Soc.*, 2012, **134**, 1986–1989.
117 H. Mistry, R. Reske, Z. Zeng, Z. J. Zhao, J. Greeley, P. Strasser and B. R. Cuenya, Exceptional Size-Dependent Activity Enhancement in the Electroreduction of CO_2 over Au Nanoparticles, *Chem. Soc.*, 2014, **136**, 16473–16476.
118 C. Kim, T. Eom, M. S. Jee, H. Jung, H. Kim, B. K. Min and Y. J. Hwang, Insight into Electrochemical CO_2 Reduction on Surface-Molecule-Mediated Ag Nanoparticles, *ACS Catal.*, 2017, **7**, 779–785.
119 J. M. Spurgeon and B. Kumar, A comparative technoeconomic analysis of pathways for commercial electrochemical CO_2 reduction to liquid products, *Energy Environ. Sci.*, 2018, **11**, 1536.
120 C. Kim, F. Dionigi, V. Beermann, X. Wang, T. Möller and P. Strasser, Alloy Nanocatalysts for the Electrochemical Oxygen Reduction (ORR) and the Direct Electrochemical Carbon Dioxide Reduction Reaction (CO_2RR), *Adv. Mater.*, 2019, **31**, 1805617.
121 W. Gao, Y. Xu, L. Fu, X. Chang and B. Xu, Experimental evidence of distinct sites for CO_2-to-CO and CO conversion on Cu in the electrochemical CO_2 reduction reaction, *Nat. Catal.*, 2023, **6**, 885–894.
122 Q. Wang, X. Yang, H. Zang, C. Liu, J. Wang, N. Yu, L. Kuai, Q. Qin and B. Geng, InBi Bimetallic Sites for Efficient Electrochemical Reduction of CO_2 to HCOOH, *Small*, 2023, **19**, 2303172.
123 A. R. Woldu, A. G. Yohannes, Z. Huang, P. Kennepohl, D. Astruc, L. Hu and X. C. Huang, Experimental and Theoretical Insights into Single Atoms, Dual Atoms, and Sub-Nanocluster Catalysts for Electrochemical CO_2 Reduction (CO_2RR) to High-Value Products, *Adv. Mater.*, 2024, **36**, 2414169.
124 H. Dai, T. Song, X. Yue, S. Wei, F. Li, Y. Xu, S. Shu, Z. Cui, C. Wang, J. Gu and L. Duan, Cu single-atom electrocatalyst on nitrogen-containing graphdiyne for CO_2 electroreduction to CH_4, *Chin. J. Catal.*, 2024, **64**, 123–132.
125 B. Wang, M. Wang, Z. Fan, C. Ma, S. Xi, L. Y. Chang, M. Zhang, N. Ling, Z. Mi, S. Chen, W. R. Leow, J. Zhang, D. Wang and Y. Lum, Nanocurvature-induced field effects enable control over the activity of single-atom electrocatalysts, *Nat. Commun.*, 2024, **15**, 1719.
126 R. Purbia, S. Y. Choi, C. H. Woo, J. Jeon, C. Lim, D. K. Lee, J. Y. Choi, H.-S. Oh and J. M. Baik, Highly selective and low-overpotential electrocatalytic CO2 reduction to ethanol by Cu-single atoms decorated N-doped carbon dots, *Appl. Catal., B*, 2024, **345**, 123694.
127 S. Cui, C. Yu, X. Tan, W. Li, Y. Zhang and J. Qiu, A tandem catalyst with high CO_2 capture capability to achieve a promoted CO_2-to-CH_4 electrochemical conversion, *Chem. Eng. J.*, 2023, **470**, 144083.
128 J. Ding, B. H. Yang, X. L. Ma, S. Liu, W. Liu, Q. Mao, Y. Huang, J. Li, T. Zhang and B. Liu, A tin-based tandem electrocatalyst for CO_2 reduction to ethanol with 80% selectivity, *Nat. Energy*, 2023, **8**, 1386–1394.

129 Y. Wang, S. L. Marquard, D. Wang, C. Dares and T. J. Meyer, Single-Site, Heterogeneous Electrocatalytic Reduction of CO_2 in water as the Solvent, *ACS Energy Lett.*, 2017, **2**, 1395–1399.
130 S. Baskaran and Y. Jung, Mo_2CS_2-MXene supported single-atom catalysts for efficient and selective CO_2 electrochemical reduction, *Appl. Surf. Sci.*, 2022, **592**, 153339.
131 D. Zhao, Z. Chen, W. Yang, S. Liu, X. Zhang, Y. Yu, W. C. Cheong, L. Zheng, F. Ren, G. Ying, *et al.*, MXene (Ti_3C_2) vacancy-confined single-atom catalyst for efficient functionalization of CO_2, *J. Am. Chem. Soc.*, 2019, **141**, 4086–4093.
132 W. Liu, H. Li, P. Ou, J. Mao, L. Han, J. Song, J. Luo and H. L. Xin, Isolated Cu-Sn diatomic sites for enhanced electroreduction of CO_2 to CO, *Nano Res.*, 2023, **16**, 8729–8736.
133 L. Zhang, J. Feng, L. Wu, X. Ma, X. Song, S. Jia, X. Tan, X. Jin, Q. Zhu, X. Kang, J. Ma, *et al.*, Oxophilicity-controlled CO_2 electroreduction to C_{2+} alcohols over Lewis acid metal-doped $Cu^{\delta+}$ catalysts, *J. Am. Chem. Soc.*, 2023, **145**, 21945–21954.
134 X. Su, Y. Sun, L. Jin, L. Zhang, Y. Yang, P. Kerns, B. Liu, S. Li and J. He, Hierarchically porous Cu/Zn bimetallic catalysts for highly selective CO_2 electroreduction to liquid C_2 products, *Appl. Catal., B*, 2020, **269**, 118800.
135 G. Chen, J. Fu, B. Liu, C. Cai, H. Li, Z. Zhang, K. Liu, Z. Lin and M. Liu, Passivation of Cu nanosheet dissolution with Cu^{2+}-containing electrolytes for selective electroreduction of CO_2 to CH_4, *Environ. Sci.:Nano*, 2022, **9**, 3312–3317.
136 Z. Xu, Y. Xie and Y. Wang, Pause electrolysis for acidic CO_2 reduction on 3-dimensional Cu, *Mater. Rep. Energy*, 2023, **3**, 100173.
137 M. Fan, J. E. Huang, R. K. Miao, Y. Mao, P. Ou, F. Li, X. Y. Li, Y. Cao, Z. Zhang, J. Zhang, *et al.*, Cationic-group-functionalized electrocatalysts enable stable acidic CO_2 electrolysis, *Nat. Catal.*, 2023, **6**, 763–772.
138 S. Cao, H. Chen, X. Wei, J. Li, C. Yang, Z. Chen, S. Wei, S. Liu, Z. Wang and X. Lu, Asymmetric coordination engineering of active centers in MXene-based single atom catalysts for high-performance ECO_2RR, *Carbon*, 2024, **225**, 119094.
139 S. Chen, T. Luo, X. Li, K. Chen, Q. Wang, J. Fu, K. Liu, C. Ma, Y.-R. Lu, H. Li, K. S. Menghrajani, C. Liu, S. A. Maier, T.-S. Chan and M. Liu, Design of reaction-driven active configuration for enhanced CO_2 electroreduction, *Nano Energy*, 2024, **128**, 109873.
140 Z. Lv, C. Wang, Y. Liu, R. Liu, F. Zhang, X. Feng, W. Yang and B. Wang, Improving CO_2-to-C_2 Conversion of Atomic CuFONC Electrocatalysts through F, O-Codrived Optimization of Local Coordination Environment, *Adv. Energy Mater.*, 2024, **14**, 2400057.
141 S. Yang, H. Wang, Y. Xiong, M. Zhu, J. Sun, M. Jiang, P. Zhang, J. Wei, Y. Xing, Z. Tie and Z. Jin, Ultrafast Thermal Shock Synthesis and Porosity Engineering of 3D Hierarchical Cu–Bi Nanofoam Electrodes for Highly Selective Electrochemical CO_2, *Nano Lett.*, 2023, **23**, 10140–10147.
142 Z. Wang, J. Yang, Z. Song, M. Lu, W. Wang, Z. Ren and Z. Chen, Reprogramming the Microenvironment of Cobalt Phthalocyanine by a Targeted Multifunctional π-Conjugated Modulator Enables Concerted CO_2 Electroreduction, *ACS Catal.*, 2024, **14**, 8138–8147.
143 J. Lei and T. Zhu, Impact of Potential and Active-Site Environment on Single-Iron-Atom-Catalyzed Electrochemical CO_2 Reduction from Accurate Quantum Many-Body Simulations, *ACS Catal.*, 2024, **14**, 3933–3942.
144 A. Kumar, M. Ubaidullah, P. V. Pham and R. K. Gupta, Three-dimensional macro-structures of graphene-based materials for emerging heterogeneous electrocatalysis: Concepts, syntheses, principles, applications, and perspectives, *Chem. Eng. J.*, 2024, **499**, 156664.
145 J. M. Gracia, F. F. Prinsloo and J. W. Niemantsverdriet, Mars-van Krevelen-like Mechanism of CO Hydrogenation on an Iron Carbide Surface, *Catal. Lett.*, 2009, **133**, 257–261.
146 J. Chai, R. Pestman, W. Chen, N. Donkervoet, A. I. Dugulan, Z. Men, P. Wang and E. J. M. Hensen, Isotopic Exchange Study on the Kinetics of Fe Carburization and the Mechanism of the Fischer-Tropsch Reaction, *ACS Catal.*, 2022, **12**, 2877–2887.
147 L. Brübach, D. Hodonj and P. Pfeifer, Kinetic Analysis of CO_2 Hydrogenation to Long-Chain Hydrocarbons on a Supported Iron Catalyst, *Ind. Eng. Chem. Res.*, 2022, **61**, 1644–1654.
148 Y. Sun, G. Yang, M. Xu, J. Xu and Z. Sun, A simple coupled ANNs–RSM approach in modeling product distribution of Fischer–Tropsch synthesis using a microchannel reactor with Ru–promoted Co/Al_2O_3 catalyst, *Int. J. Energy Res.*, 2020, **44**, 1046–1061.
149 Y. Wang, J. Hu, X. Zhang, A. Yusuf, B. Qi, H. Jin, Y. Liu, J. He, Y. Wang, G. Yang and Y. Sun, Kinetic Study of Product Distribution Using Various Data-Driven and Statistical Models for Fischer-Tropsch Synthesis, *ACS Omega*, 2021, **6**, 27183–27199.
150 Q. Zhang, L. Guo and Z. Hao, CO hydrogenation on M_1/W_6S_8 (M = Co and Ni) single-atom catalysts: Competition between C_2 hydrocarbons and methanol synthesis pathways, *Mol. Catal.*, 2019, **464**, 10–21.
151 X. Wang, X. P. Fu, W. Z. Yu, C. Ma, C. J. Jia and R. Si, Synthesis of a ceria-supported iron–ruthenium oxide catalyst and its structural transformation from subnanometer clusters to single atoms during the Fischer–Tropsch synthesis reaction, *Inorg. Chem. Front.*, 2017, **4**, 2059–2067.